

---

# Distributed Event-Based Learning via ADMM

---

**Guener Dilsad ER**

Learning and Dynamical Systems Group  
Max Planck Institute for Intelligent Systems  
72076 Tübingen, Germany  
guenerdilsad.er@tuebingen.mpg.de

**Sebastian Trimpe**

Institute for Data Science in Mechanical Eng.  
RWTH Aachen University  
52068 Aachen, Germany  
trimpe@dsme.rwth-aachen.de

**Michael Muehlebach**

Learning and Dynamical Systems Group  
Max Planck Institute for Intelligent Systems  
72076 Tübingen, Germany  
michaelm@tuebingen.mpg.de

## Abstract

We consider a distributed learning problem, where agents minimize a global objective function by exchanging information over a network. Our approach has two distinct features: (i) It substantially reduces communication by triggering communication only when necessary, and (ii) it is agnostic to the data-distribution among the different agents. We can therefore guarantee convergence even if the local data-distributions of the agents are arbitrarily distinct. We analyze the convergence rate of the algorithm and derive accelerated convergence rates in a convex setting. We also characterize the effect of communication drops and demonstrate that our algorithm is robust to communication failures. The article concludes by presenting numerical results from a distributed LASSO problem, and distributed learning tasks on MNIST and CIFAR-10 datasets. The experiments underline communication savings of 50% or more due to the event-based communication strategy, show resilience towards heterogeneous data-distributions, and highlight that our approach outperforms common baselines such as FedAvg, FedProx, and FedADMM.

## 1 Introduction

Distributed learning refers to the minimization of a global objective function over a network of agents, where each agent has only access to a local cost function and can communicate with some or all agents in the network. Distributed learning systems provide a solution for handling the growing amount of data being generated everywhere on earth, by utilizing the computational power of individual devices in a network rather than relying on a central entity. This takes the burden off central processors and improves data privacy by avoiding a centralized training and storage of raw data.

Distributed learning is particularly challenging when the data is not independent and identically distributed (non-i.i.d.) across the different agents. This situation often hinders the convergence to a globally optimal model. The non-i.i.d. nature leads to disparities in local datasets, preventing the local models from generalizing across the entire dataset, leading to a fundamental dilemma between minimizing local and global objective functions [Acar et al., 2021]. In addition, a second key challenge arises from the communication between agents, which is required to ensure convergence to the global solution and may lead to a substantial overhead. This communication overhead results in a waste of energy [Li et al., 2020b], and is prone to delays and communication channel drops.

As a result, both, non-i.i.d. datasets and communication overhead, constitute major bottlenecks for enabling large-scale learning systems.

We provide an effective solution to both challenges. Inspired by the sent-on-delta concept [Miskowicz, 2006], we reduce the communication load by introducing an event-based communication strategy, such that each agent (or computational node) communicates only if necessary. We further base our approach on the Alternating Direction Method of Multipliers (ADMM). Our method is therefore robust against ill-conditioning and agnostic towards a disparity of the local data-distributions among the agents (these can be skewed in arbitrary ways). The approach further enables an explicit trade-off between communication load on the network and solution accuracy via a small set of hyperparameters that have a clear interpretation. We explicitly quantify the influence of these hyperparameters on the solution accuracy and analyze the effect of communication drops. The article concludes by highlighting the effectiveness of our algorithm in training neural networks, and solving LASSO problems in a distributed and communication-efficient manner.

Our theoretical analysis builds on a recent trend in the optimization literature [Wibisono et al., 2016, Su et al., 2016, Muehlebach and Jordan, 2019, Tong and Muehlebach, 2023] that views algorithms as dynamical systems and leverages ideas from differential or symplectic geometry, as well as passivity and dissipativity [Lessard et al., 2016, Muehlebach and Jordan, 2020]. As we will show, this enables convergence proofs and a convergence rate analysis for our distributed algorithms, together with an analysis of robustness against communication drops. Our work provides important insights into the behavior of the event-based optimization under communication drops, an aspect, which has been overlooked in prior works, and lays thereby the groundwork for future research in this area.

**Related Work:** In the 1980s, the work by Bertsekas and Tsitsiklis [1989] and others laid the foundation for the analysis of distributed algorithms. As machine learning became popular, distributed learning emerged, specifically focusing on parallelizing computation for empirical risk minimization. Shokri and Shmatikov [2015] explored collaborative deep learning with multiple agents using distributed stochastic gradient descent, which was later coined federated learning [McMahan et al., 2017, Kairouz et al., 2021, Asad et al., 2023]. Thus, the consensus problem, where agents are required to agree on a common value or decision, provides a unifying link between federated and distributed learning, and is also a special instance of distributed optimization [Wei and Ozdaglar, 2012].

The trade-off between communication versus computation is inevitable in distributed optimization [Nedic et al., 2018]. Recent work by Cao et al. [2023] categorizes communication-efficient distributed learning into four main strategies: (1) minimizing the number of communications, (2) compressing data, (3) managing resources (e.g., bandwidth), and (4) using game theoretical approaches. We focus our review on the first category that aligns with our work, and reduces communication by transmitting information only if necessary. A first line of work [McMahan et al., 2017, Wei Liu et al., 2021, Reisizadeh et al., 2020, and many more] proposes algorithms with a periodical exchange of model parameters either among all agents or among randomly selected agents for decreasing communication load. While this approach is particularly straightforward to implement and easy to understand, the random sampling might miss important changes or perform unnecessary communications of the model parameters. A second line of work involves accelerated gradient methods for distributed optimization, reducing the need for many communication rounds to converge. Kovalev et al. [2020] and Nabli and Oyallon [2023] introduce methods that optimize the number of gradient evaluations together with communication rounds. Shamir et al. [2014] replaces gradient descent with Newton-like methods and Hendrikx et al. [2020] proposes statistical preconditioning – both methods further improve convergence rates at the cost of a higher computational load per iteration. There has also been a third line of work that focuses on reducing communication via event-based triggering and compression of network parameters [Liu et al., 2019, Singh et al., 2023, Zhang et al., 2023]. While [Zhang et al., 2024, 2023] employ an ADMM-based strategy that is similar to ours, their focus lies on investigating different compression schemes, and not on analyzing convergence rates and the effect of communication drops. A somewhat similar approach has been proposed by Liu et al. [2021] and relies on a lazy evaluation of dual gradients to reduce communication.

In addition to the communication overhead, another major challenge for distributed learning arises from non-i.i.d. data distributions over the individual agents [Zhao et al., 2018, Li et al., 2020c]. Recent contributions by Li et al. [2020a], Acar et al. [2021], Shi et al. [2023] add a proximal regularization term to the local objective functions of the individual agents, whereas Zhang et al. [2021] (FedPD) and Zhou and Li [2023], Wang et al. [2022], Gong et al. [2022] (FedADMM) address the challenge

with ADMM formulations. However, compared to our work, FedADMM [Zhou and Li, 2023, Wang et al., 2022, Gong et al., 2022] relies on utilizing a random selection of agents that communicate and FedPD [Zhang et al., 2021] considers full participation, whereas we use an event-triggered mechanism. As we also highlight in numerical experiments, a random selection of agents might prevent important local changes from propagating quickly through the network, leading to a slower convergence. To the best of our knowledge, this is the first work to provide a convergence analysis of distributed learning with event-triggered communication that addresses key aspects, such as packet drop and the presence of non-i.i.d. data.

**Contributions:** Our contributions are summarized as follows:

(i) We propose event-based communication for distributed optimization, where a communication event is only triggered, when the current state has deviated by a predefined threshold  $\Delta$ , indicating a significant change in the local decision variables. As we will show, our approach is effective in reducing communication overhead and can adapt to the limited communication resources in heterogeneous networks.

(ii) We characterize the effect of the communication threshold  $\Delta$  on the solution accuracy and therefore quantify the trade-off between communication and solution accuracy. Compared to other ADMM-based approaches, such as [Zhang et al., 2021, Zhou and Li, 2023], our method is versatile, both in the selection of variables that are being communicated (which is important for reducing communication in practice), as well as the different problem formulations that we can address. In particular, our approach goes beyond the scope of consensus problems, and can solve generic constrained optimization problems, sparse regression and LASSO problems, perform robust principal component analysis [Candès et al., 2011], and solve distributed learning instances where the features but not the data points are distributed [Boyd et al., 2010].

(iii) Numerical experiments support our theoretical analysis and highlight that our approach even converges in the most extreme non-i.i.d. setting, where each agent has only access to training data from a single class. A comparison to the baselines FedADMM [Zhou and Li, 2023], FedProx [Li et al., 2020a] and FedAvg [McMahan et al., 2017] demonstrate superiority both in terms of communication efficiency, as well as in classification accuracy.

(iv) We demonstrate an accelerated convergence rate, and derive symbolic expressions that relate the convergence rate to instance-specific quantities such as the condition number and the topology of the communication network. The convergence analysis requires a Lyapunov-like function that is different compared to [Nishihara et al., 2015], due to the presence of the event-based communication.

(v) We study the robustness of our algorithm against communication drops, both in theory as well as in numerical experiments, which, we believe, is largely missing in the literature (a notable exception for the consensus problem is [Bastianello et al., 2021]). We address communication drops algorithmically by proposing a periodic reset strategy. Without such a reset strategy, inter-agent errors accumulate rapidly in the presence of drops and prevent convergence.

**Outline:** The article is structured as follows: Sec. 2 describes the problem formulation and introduces our event-based learning algorithm in the consensus setting. The more general formulation is discussed in Sec. 3, where we also introduce a dynamical systems model for our algorithm. Sec. 4 discusses the convergence analysis of the proposed algorithm and presents convergence rates, while empirical results that underline the theoretical findings are included in Sec. 5 and in App. F. The appendix contains additional technical details about the communication structure in App. A and the details of the convergence analysis in App. B and App. C.

## 2 Event-Based Distributed Learning

Distributed learning aims at solving

$$\min_{x \in \mathbb{R}^n} \sum_{i=1}^N f^i(x),$$

where the overall cost function  $f(x)$  is the sum of  $N$  individual, potentially nonsmooth functions. The different  $f^i$  typically arise from different training datasets stored on different computational

---

**Algorithm 1** Event-Based Distributed Learning with Over-Relaxed ADMM
 

---

**Require:**  $f^i$ , parameters  $\rho, \Delta^d, \Delta^z$ , reset period  $T$

**Require:** Initialize  $\hat{x}_0^i = x_0, \hat{z}_0 = \zeta_0 = x_0, \hat{u}_{-1}^i = u_0^i$

```

for  $k = 0$  to  $t_{\max}$  do
  for  $i = 1$  to  $N$  do
     $\hat{z}_k^i \leftarrow$  event-based receive of  $z_{k+1} - z_{[k]}$  {Agent  $i$ }
     $u_k^i = u_{k-1}^i + \alpha x_k^i - \hat{z}_k^i + (1 - \alpha)\hat{z}_{k-1}^i$ 
     $x_{k+1}^i = \arg \min_{x^i} f^i(x^i) + \frac{\rho}{2}|x^i - \hat{z}_k^i + u_k^i|^2$ 
    event-based send of  $d_{k+1}^i - d_{[k]}^i$  where  $d_{k+1}^i = \alpha x_{k+1}^i + u_k^i$ 
  end for
   $\hat{\zeta}_k \leftarrow$  event-based receive of  $d_{k+1}^i - d_{[k]}^i$  {Agent  $N+1$ }
   $z_{k+1} = \arg \min_z g(z) + \frac{N\rho}{2}|z - \hat{\zeta}_k + (1 - \alpha)z_k|^2$ 
  event-based send of  $z_{k+1} - z_{[k]}$ 
  if  $\text{mod}(k+1, T) = 0$  then
    perform reset  $\rightarrow \hat{\zeta}_k = \zeta_k, \hat{z}_k = z_k$ 
  end if
end for

```

---

nodes. In the most basic instance, our algorithm arises from the consensus formulation

$$\min_{x^1, \dots, x^N \in \mathbb{R}^n} \sum_{i=1}^N f^i(x^i) + g(z), \quad \text{subject to } x^i = z, \quad i = 1, \dots, N, \quad (1)$$

where we will impose the constraints  $x^i = z$  by corresponding dual variables  $u^i$ . Thus, by guaranteeing constraint satisfaction, we can handle arbitrary non-i.i.d. data distributions among the different computational nodes. In addition, we assume the function  $f^i: \mathbb{R}^n \rightarrow \mathbb{R}$  to be smooth, while  $g: \mathbb{R}^n \rightarrow \bar{\mathbb{R}}$  is allowed to be nonsmooth ( $g$  typically represents an indicator function of the feasible set) and maps to the extended real numbers  $\bar{\mathbb{R}}$ .

Our event-based algorithm, stated in Alg. 1, works as follows. Each agent (or computational node)  $i$ ,  $i = 1, \dots, N$ , has access to the local objective function  $f^i$ , his local solution  $x^i$ , his local multiplier  $u^i$ , and an estimate  $\hat{z}^i$  of the consensus variable  $z$ . We further introduce the agent  $N+1$  (acting as server) that has access to  $g$ , the variable  $z$ , and maintains an estimate  $\hat{\zeta}$  of the average

$$\zeta_k := \frac{1}{N} \sum_{i=1}^N \alpha x_{k+1}^i + u_k^i.$$

Following the communication structure in Fig. 1, the algorithm proceeds in two steps:

**i) Parallel update of agents  $i = 1, \dots, N$ :** Each agent  $i = 1, \dots, N$  first updates his estimate  $\hat{z}_k^i$  based on whether it receives an event-based communication from the agent  $N+1$ . The agent then updates his multiplier  $u_k^i$  and solves a local minimization over  $f^i$ , which also includes a quadratic regularization term. The regularization term ensures that the minimization is well-conditioned (a key advantage to dual ascent, for example) and the local solution  $x^i$  is biased towards  $\hat{z}_k^i$ . In practice, the minimization is replaced by a fixed number of (stochastic) gradient descent steps. If the resulting value  $d_{k+1}^i := \alpha x_{k+1}^i + u_k^i$  of the agent  $i$  is significantly different from the value that it last communicated to the agent  $N+1$ , an event-based communication is triggered and the difference of  $d_{k+1}^i$  to the last communicated value is sent to the agent  $N+1$ .

**ii) Update of agent  $N+1$ :** The agent  $N+1$  updates his estimate  $\hat{\zeta}$  of  $\zeta$  by accumulating the  $d^i$  variables that it receives from all agents. It then updates the consensus variable  $z_{k+1}$  by solving a local minimization over  $g$  with a quadratic regularization term. Note that if the nonsmooth component  $g$  is missing,  $z_{k+1}$  is simply set to  $\hat{\zeta}_k - (1 - \alpha)z_k$ . Finally, the agent  $N+1$  triggers an event-based communication if the value  $z_{k+1}$  is significantly different from the value that it last communicated to the agents  $i = 1, \dots, N$ .

The remainder of this section explains the details of the event-based communication protocol on the example of the communication of  $d^i$ , which is related to the primal  $x^i$  and dual  $u^i$  variables of agent  $i$ .

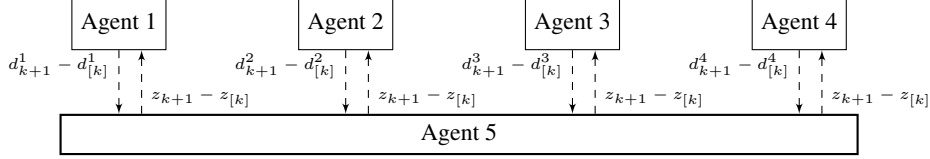


Figure 1: The figure illustrates the distributed learning setup. The Agents 1–4 store  $x^i, u^i$  and perform updates based on the information received by Agent 5, according to Alg. 1. Agent 5, stores  $z$  and performs updates based on the information received by Agent 1–4.

The other event-based communications proceed in a similar way. The protocol comes in two variants, **vanilla event-based** and **randomized event-based**.

**Vanilla event-based:** A communication is triggered, if the value  $d_{k+1}^i$  has deviated by more than the predefined threshold  $\Delta^d > 0$  compared to the value that was last communicated. We introduce the variable  $d_{[k]}^i$  to denote the value  $d_k^i$  that was last communicated and add the index  $i$  to the set  $\mathcal{C}_{k+1}^d$ . The set  $\mathcal{C}_{k+1}^d$  denotes the set of agents that trigger a communication of  $d_{k+1}^i$  at time-step  $k$ , that is,

$$|d_{k+1}^i - d_{[k]}^i| > \Delta^d \iff i \in \mathcal{C}_{k+1}^d,$$

and  $d_{k+1}^i - d_{[k]}^i$  is sent out. We also model communication drops, which we represent by the variables  $\chi_{k+1}^{di}$ . The variable  $\chi_{k+1}^{di}$  takes the value  $\chi_{k+1}^{di} = -(d_{k+1}^i - d_{[k]}^i)$ , if  $d_{k+1}^i - d_{[k]}^i$  is not received by the agent  $N+1$ ; otherwise  $\chi_{k+1}^{di} = 0$ . The agent  $N+1$  updates his estimate of the average  $\zeta_k$  according to the primal and dual variables that it has received at time  $k$ , that is,

$$\hat{\zeta}_k = \hat{\zeta}_{k-1} + \frac{1}{N} \sum_{i \in \mathcal{C}_{k+1}^d} d_{k+1}^i - d_{[k]}^i + \chi_{k+1}^{di}.$$

**Randomized event-based:** The protocol makes a case distinction. If  $|d_{k+1}^i - d_{[k]}^i| \leq \Delta^d$ , a communication is randomly triggered with probability  $p_{\text{trig}}$ . If  $|d_{k+1}^i - d_{[k]}^i| > \Delta^d$ , a communication is triggered with certainty. The rest of the communication protocol is analogous to **vanilla event-based**. We observed in our numerical experiments that **randomized event-based** often improves **vanilla event-based** in terms of the achieved communication versus solution accuracy trade-off.

The error caused by the event-based communication remains bounded at all times thanks to the communication protocol and the periodic resets. This is summarized with the next proposition:

**Proposition 2.1.** *The error  $\hat{\zeta}_k - \zeta_k$  at iteration  $k$  is bounded by  $|\hat{\zeta}_k - \zeta_k| \leq \Delta^d + T\bar{\chi}^d$ , where  $T$  denotes the reset period (see Alg. 1) and  $\bar{\chi}^d$  is a bound on the disturbance  $\chi_k^{di}$ .*

*Proof.* We note that the error  $\hat{\zeta}_k - \zeta_k$  can be expressed as

$$\frac{1}{N} \sum_{i=1}^N \underbrace{(d_{[k+1]}^i - d_{k+1}^i)}_{\text{I}} + \underbrace{\sum_{l=T_{[k]}}^k \chi_{l+1}^{di}}_{\text{II}},$$

where  $T_{[k]}$  denotes the last time instant where a reset has been performed. The terms I and II have each a clear interpretation: In the absence of communication drops,  $\hat{\zeta}$  is an average over the primal and dual variables,  $x_{[k+1]}^i$  and  $u_{[k]}^i$ , that were last communicated, which leads to the term I. The term II captures the communication drops. The communication protocol ensures that  $|d_{k+1}^i - d_{[k+1]}^i| \leq \Delta^d$ , for all  $k \geq 0$ , which means that the term I is bounded by  $\Delta^d$ . The bound for the term II arises from the triangle inequality, which yields,  $\bar{\chi}^d$  and concludes the proof.  $\square$

The previous proposition required the variable  $\chi_{k+1}^{di}$  to be bounded. Prop. D.1 in App. D establishes such a bound under standard conditions on  $f$  and  $g$ .

We now state the main convergence result for Alg. 1. The result arises as a corollary from the convergence analysis in the more general distributed optimization setting (see Thm. 4.1).

**Corollary 2.2.** *Let  $f$  be  $m$ -strongly convex and  $L$ -smooth with  $\kappa = L/m$ . Let the step-size be  $\rho = (mL)^{\frac{1}{2}}\kappa^\epsilon$  with  $\epsilon \in [0, \infty)$ , and let the relaxation parameter  $\alpha = 1$ . For large enough  $\kappa$ , we have*

$$|z_k - z_*|^2 + \frac{1}{N} \sum_{i=1}^N |u_k^i - u_*^i|^2 \leq 4 \left(1 - \frac{1}{4\kappa^{\epsilon + \frac{1}{2}}}\right)^{2k} \left( |z_0 - z_*|^2 + \frac{1}{N} \sum_{i=1}^N |u_0^i - u_*^i|^2 \right) + \frac{5}{N} \kappa^{2+2\epsilon} \Delta^2,$$

where  $z_*$  and  $u_*^i$  are the optimal values for the consensus variable  $z$  and the dual variables associated with each agent, and  $\Delta = \Delta^d + \Delta^z + T(\bar{\chi}^d + \bar{\chi}^z)$  captures the error arising from the event-based communication.

The convergence result bounds the distance between the consensus variable  $z_k$  to the optimal solution  $z_* = x_*$  that minimizes (1). Our analysis is based on modeling our event-based learning algorithm as a dynamical system, whereby the event-based communication strategy contributes to additional disturbances, which, by virtue of the communication protocol, are guaranteed to be bounded. The next section explains the formulation of our algorithm as a dynamical system.

### 3 Event-Based ADMM as a Dynamical System

We consider a constrained minimization problem which generalizes (1) as follows:

$$\min_{x \in \mathbb{R}^p, z \in \mathbb{R}^q} f(x) + g(z), \quad \text{subject to } Ax + Bz = c, \quad (2)$$

where  $x \in \mathbb{R}^p$  and  $z \in \mathbb{R}^q$  are decision variables,  $A \in \mathbb{R}^{r \times p}$ ,  $B \in \mathbb{R}^{r \times q}$ , and  $c \in \mathbb{R}^r$  are corresponding matrices, and the objective function is decomposed into a smooth part  $f: \mathbb{R}^p \rightarrow \mathbb{R}$  and a nonsmooth part  $g: \mathbb{R}^q \rightarrow \bar{\mathbb{R}}$ . We will provide an analysis under the following assumptions.

**Assumption 1.** *The matrix  $A$  is invertible and  $B$  is full column rank.*

**Assumption 2.** *The function  $f$  is  $m$ -strongly convex and  $L$ -smooth. The function  $g$  is convex.*

The general formulation (2) provides a versatile framework for addressing a broad spectrum of distributed optimization problems, such as consensus and resource sharing, as well as distributed model fitting, see for example [Boyd et al., 2010]. App. A further highlights how the general formulation can be tailored and simplified to accommodate specific applications, such as the sharing problem or finding a consensus on a graph.

Our event-based distributed learning method is summarized in Alg. 2. The algorithm is based on an over-relaxed version of ADMM, where an event-based communication structure between different agents is introduced. The over-relaxation brings the additional parameter  $\alpha$ , which, as we will show, can be used to achieve faster convergence rates. The communication structure of the algorithm is shown in Fig. 2 and includes three agents that keep track of the individual quantities  $r_k = Ax_k$ ,  $s_k = Bz_k$ , and the dual multiplier  $u_k$ . In the special case of the consensus problem, the updates of the primal variable  $x_k$  and dual variable  $u_k$  decompose further into local updates based on  $x_k^i$  and  $u_k^i$ , which results in the communication structure shown in Fig. 1.

Alg. 2 begins by initializing its variables, and over a series of iterations, agents alternate between sharing information and optimizing their local variables. Key steps include updating variables based on local objectives and residuals, and triggering communication events when individual residual changes exceed predefined thresholds. The algorithm leverages event-based communication to reduce the communication load, while still achieving convergence towards an optimal solution of (2), as we will show in the following section. The event-based communication proceeds as in Sec. 2, that is, the  $r$ -agent, for example, triggers a communication with the other agents if  $|r_{k+1} - r_{[k]}| > \Delta^r$ , at which point it sends the difference  $r_{k+1} - r_{[k]}$  to the other agents. We again model communication drops by introducing the variables  $\chi_{k+1}^{ru}$  if the communication is not received by the  $u$ -agent at time  $k+1$ . The notation is analogous for the remaining agents and communication lines (see also Fig. 2).

Alg. 2 has three update steps that occur sequentially, whereby the first two involve optimization problems that can be replaced by their corresponding stationarity conditions. This yields the following implicit update equations:

$$\begin{aligned} 0 &= \nabla f(x_{k+1}) + \rho A^\top (Ax + \hat{s}_k^r - c + \hat{u}_k^r) \\ 0 &\in \partial g(z_{k+1}) + \rho B^\top (\alpha \hat{r}_{k+1}^s - (1 - \alpha)Bz_k + Bz_{k+1} - \alpha c + \hat{u}_k^s) \\ u_{k+1} &= u_k + \alpha \hat{r}_{k+1}^u - (1 - \alpha)\hat{s}_k^u + \hat{s}_{k+1}^u - \alpha c, \end{aligned}$$

---

**Algorithm 2** Event-Based Distributed Optimization with Over-Relaxed ADMM
 

---

**Require:** Functions  $f$  and  $g$ , matrices  $A$  and  $B$ , vector  $c$ , parameters  $\rho$  and  $\alpha$

**Require:** Initial condition  $x_0, z_0$

$$r_0 = \hat{r}_0^s = \hat{r}_0^u = Ax_0, \quad s_0 = \hat{s}_0^r = \hat{s}_0^u = Bz_0, \quad u_0 = \hat{u}_0^r = \hat{u}_0^s = 0$$

**for**  $k = 0$  to  $t_{\max}$  **do**

$$\hat{s}_k^r, \hat{u}_k^r \leftarrow \text{event-based receive of } s_{k+1} - s[k], u_{k+1} - u[k]$$

$$x_{k+1} = \arg \min_x f(x) + \frac{\rho}{2} \|Ax + \hat{s}_k^r - c + \hat{u}_k^r\|^2 \quad \{\text{r-agent}\}$$

$$\text{event-based send of } r_{k+1} - r[k] \text{ where } r_{k+1} = Ax_{k+1}$$

$$\hat{r}_{k+1}^s, \hat{u}_k^s \leftarrow \text{event-based receive of } r_{k+1} - r[k], u_{k+1} - u[k]$$

$$z_{k+1} = \arg \min_z g(z) + \frac{\rho}{2} \|\alpha \hat{r}_{k+1}^s - (1 - \alpha)Bz_k + Bz - \alpha c + \hat{u}_k^s\|^2 \quad \{\text{s-agent}\}$$

$$\text{event-based send of } s_{k+1} - s[k] \text{ where } s_{k+1} = Bz_{k+1}$$

$$\hat{r}_{k+1}^u, \hat{s}_{k+1}^u \leftarrow \text{event-based receive of } r_{k+1} - r[k], s_{k+1} - s[k]$$

$$u_{k+1} = u_k + \alpha \hat{r}_{k+1}^u - (1 - \alpha)\hat{s}_{k+1}^u + \hat{s}_{k+1}^u - \alpha c \quad \{\text{u-agent}\}$$

$$\text{event-based send of } u_{k+1} - u[k]$$

**if**  $\text{mod}(k + 1, T) = 0$  **then**

$$\text{reset} \rightarrow \hat{r}_{k+1}^{u;s} = r_{k+1}, \hat{s}_{k+1}^{u;r} = s_{k+1}, u_{k+1}^{r;s} = u_{k+1}$$

**end if**

**end for**

---

which can be expressed by the dynamical system shown in Fig. 2. We note that the variable  $x_{k+1}$  is uniquely determined by  $\hat{s}_k^r$  and  $\hat{u}_k^r$  and does not depend on  $x_k$ , which means that only  $\xi_k := (s_k, u_k)$  comprises the state of the dynamical system. We further note that the dynamical system includes a nonlinear component, which arises from the gradient evaluations  $\nabla f$  and  $\partial g$ , and the system is subjected to external disturbances  $e_k$  that arise from the event-based communication. The detailed derivation and the corresponding matrices for the dynamics in Fig. 2 are included in App. B. Our convergence analysis will build on the dynamical systems model of Alg. 2. While our analysis is inspired by earlier works, such as [Nishihara et al., 2015] and [Lessard et al., 2016], the Lyapunov function that is used to prove convergence rates are different due to the external disturbances caused by the event-based communication.

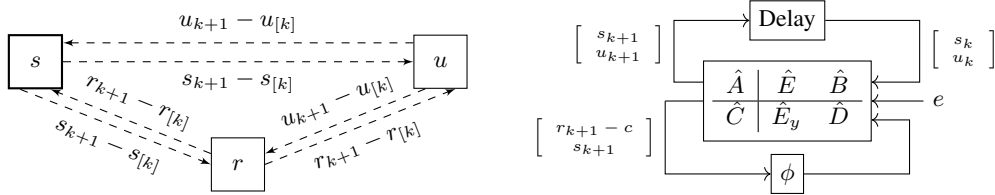


Figure 2: The figure visualizes the event-based communication structure of Alg. 2 on the left and a discrete-time dynamical system which represents the sequence generated by the event-based ADMM algorithm on the right. The function  $\phi$  is nonlinear and represents the evaluation of gradients.

## 4 Convergence Analysis

This section provides convergence guarantees for the event-based learning algorithm (Alg. 2).

**Theorem 4.1.** *Let Assmp. 1 and 2 be satisfied and let the step-size for Alg. 2 be  $\rho = \kappa^\epsilon \sqrt{mL}/(\underline{\sigma}(A)\bar{\sigma}(A))$ , for some  $\epsilon \geq 0$  and  $\alpha \in (0.675, 1 + \sqrt{1 - 1/\sqrt{\kappa}})$ ,  $\kappa = L\bar{\sigma}^2(A)/(m\sigma^2(A))$ , where  $\underline{\sigma}$  and  $\bar{\sigma}$  denote the minimum and maximum singular value of a matrix, respectively. Then, for large enough  $\kappa$ , the following bound holds:*

$$|\xi_k - \xi_*|^2 \leq \kappa_P |\xi_0 - \xi_*|^2 \left(1 - \frac{\alpha}{4\kappa^{\epsilon + \frac{1}{2}}}\right)^{2k} + \frac{60\kappa^{2+2\epsilon}}{\alpha(1 - |\alpha - 1|)} \Delta^2,$$

with  $\xi_k = (s_k, u_k)$ , and where  $s_k = Bz_k$ ,  $u_k$  is the dual variable, and  $\xi_*$  the optimizer corresponding to (2). Furthermore,  $\Delta = \Delta^r + \Delta^s + \Delta^u + T(\bar{\chi}^r + \bar{\chi}^s + \bar{\chi}^u)$  represents the error arising from the event-based communication and  $\kappa_P = (2\sqrt{\kappa} - 1 + \sqrt{4\kappa(\alpha - 1)^2 + 1}) / (2\sqrt{\kappa} - 1 - \sqrt{4\kappa(\alpha - 1)^2 + 1})$ .

*Proof.* The proof is based on Thm. C.5 in App. C, which shows that if the matrix inequality

$$0 \succeq \begin{bmatrix} (1 + \gamma^1)\hat{A}^\top P \hat{A} - \tau^2 P & \hat{A}^\top P \hat{B} \\ \hat{B}^\top P \hat{A} & (1 + \gamma^2)\hat{B}^\top P \hat{B} \end{bmatrix} + \begin{bmatrix} \hat{C}^1 & \hat{D}^1 \\ \hat{C}^2 & \hat{D}^2 \end{bmatrix}^\top \begin{bmatrix} \Lambda^1 M^1 & 0 \\ 0 & \Lambda^2 M^2 \end{bmatrix} \begin{bmatrix} \hat{C}^1 & \hat{D}^1 \\ \hat{C}^2 & \hat{D}^2 \end{bmatrix} \quad (3)$$

is satisfied for a symmetric positive definite matrix  $P$  and for positive constants  $\Lambda^1, \Lambda^2, \gamma^1, \gamma^2$ , the following bound holds

$$|\xi_k - \xi_*|^2 \leq \kappa_P |\xi_0 - \xi_*|^2 \tau^{2k} + \frac{\bar{\sigma}(Q)\Delta^2}{\underline{\sigma}(P)(1 - \tau^2)},$$

where  $\kappa_P$  denotes the condition number of  $P$  and  $Q$  is defined in App. C. In fact, the following set of parameters satisfies the linear matrix inequality (3),

$$P = \begin{bmatrix} 1 & \alpha - 1 \\ \alpha - 1 & 1 - \frac{1}{\sqrt{\kappa}} \end{bmatrix}, \quad \tau = 1 - \frac{\alpha}{4\kappa^{\epsilon + \frac{1}{2}}}, \quad \Lambda^1 = \alpha\kappa^{\epsilon - \frac{1}{2}}, \quad \Lambda^2 = \alpha, \quad \gamma^1 = \frac{\alpha}{\kappa^{\epsilon + \frac{3}{2}}}, \quad \gamma^2 = \frac{1}{\kappa}.$$

This can be checked as follows: The matrix on the right-hand side of (3) can be expressed as  $-\frac{1}{4}\kappa^{-2}\mathbb{L}$ , where  $\mathbb{L}$  is a symmetric  $4 \times 4$  matrix (compared to earlier analyses [Nishihara et al., 2015], the last row and last column is not zero). We now prove that  $\mathbb{L}$  is positive semidefinite for all sufficiently large  $\kappa$  by checking the leading principle minors, which can be expressed as polynomials in  $\kappa$ . If the leading terms of the principle minors have positive coefficients, it means that for large enough  $\kappa$ , the principle minor will indeed be positive.

The leading term for the first principle minor is given by  $6\kappa^{\frac{3}{2}-\epsilon}$  and is therefore positive. Likewise, the second principle minor is dominated by the positive term  $24(2 - \alpha)\kappa^{\frac{7}{2}-\epsilon}$ . For the third leading principle minor, there are two different cases. If  $\epsilon = 0$ , the leading term of the third leading principle minor is  $16\kappa^5(\alpha^4 - 4\alpha^3 - 4\alpha^2 + 22\alpha - 12)/\alpha$ , which is positive for  $\alpha \in (0.675, 2)$ . If  $\epsilon > 0$ , the leading term of the third principle minor becomes  $192\kappa^5(2 - \alpha)$ , which is positive for  $\alpha \in (0, 2)$ . Finally, for the fourth principle minor, there are also two different cases. If  $\epsilon = 0$ , the leading term is  $64\kappa^{\frac{13}{2}}(\alpha^4 - 4\alpha^3 - 4\alpha^2 + 22\alpha - 12)/\alpha^2$ , which is positive for  $\alpha \in (0.675, 2)$ . If  $\epsilon > 0$ , the leading term of the fourth principal minor becomes  $768\kappa^{\frac{13}{2}}(2 - \alpha)/\alpha$ , which is positive for  $\alpha \in (0, 2)$ . In conclusion, for all sufficiently large  $\kappa$ , all four leading principle minors are positive, which implies that  $\mathbb{L}$  is positive definite.

It remains to bound the second term  $\bar{\sigma}(Q)/(\underline{\sigma}(P)(1 - \tau^2))$ . We again investigate the symbolic expression, and conclude that the term is always bounded by  $60\kappa^{2+2\epsilon}/(\alpha(1 - |\alpha - 1|))$  for large enough  $\kappa$ . This concludes the proof.  $\square$

We conclude the section by highlighting a few important points.

(i) For  $\epsilon = 0, \alpha = 1$ , the bound can be considerably simplified to

$$|\xi_k - \xi_*|^2 \leq 2|\xi_0 - \xi_*|^2 \left(1 - \frac{1}{4\sqrt{\kappa}}\right)^{2k} + 60\kappa^2\Delta^2,$$

which shows that the convergence rate scales with  $1/\sqrt{\kappa}$  and is therefore accelerated. This also highlights that the same convergence rate (up to constants) can be achieved with the event-based learning algorithm stated in Alg. 1 compared to a standard ADMM algorithm. As we will show in the numerical experiments, our event-based algorithm reduces communication without any significant reduction in accuracy.

(ii) The bound from Thm. 4.1 also highlights how the communication thresholds  $\Delta$  affect the solution accuracy. In the simplified scenario with  $\epsilon = 0, \alpha = 1$  (the more general scenario follows the same rationale), the solution accuracy is bounded by  $|\xi_k - \xi_*| \leq 8\kappa\Delta$ , for large enough  $k$ . This means that the solution accuracy of Alg. 2 is proportional to the condition number  $\kappa$  and  $\Delta$ .

(iii) We can therefore easily ensure convergence, by choosing a time-varying  $\Delta = \Delta_k$  such that  $\Delta_k \rightarrow 0$ . The formal statement is included and derived in App. E. We also obtain precise nonasymptotic bounds. For example, if  $\Delta_k = \Delta_0/(k + 1)^t$  for any  $t > 0$ , we conclude that the error converges with  $\mathcal{O}(1/k^t)$  (see again App. E).

(iv) If  $f$  fails to be strongly convex, we can include a small regularizer, for example of the type  $m|x|^2/2$ . Choosing a diminishing regularizer with  $m = \mathcal{O}(1/k^2)$  and a diminishing threshold  $\Delta_k = \mathcal{O}(1/k^4)$  can be shown to result in an accelerated convergence rate of  $\mathcal{O}(1/k^2)$ .



## 5 Numerical Experiments

This section discusses the performance of Alg. 1 in numerical experiments, highlighting that Alg. 1 achieves fast convergence while reducing communication. We also investigate the trade-off between communication load and solution accuracy achieved by selecting different communication thresholds. The communication load is calculated by counting the number of triggered communications for  $T_{\max}$  number of steps and normalizing according to the full communication case.

We start by evaluating the performance of Alg. 1 on MNIST [Deng, 2012]. Further experiments (including linear regression, LASSO, training neural networks on CIFAR-10 and distributed training over a network of agents) are presented in App. F. App. F also includes hyperparameters for the experiments and discusses the effect of communication failures.

Fig. 3 shows the trade-off between the accuracy and communication load, for a neural network classifier trained over  $N = 10$  agents, where each agent  $i$  possesses only images of digit- $i$ . We conclude that with our algorithm and a well-chosen  $\Delta$  threshold, communication among agents can be greatly reduced while still achieving a high classification accuracy on the entire dataset (with all labels) even though the local datasets include only one label for each agent. During training, the objective is to minimize the overall loss across the entire training set, even though individual agents only hold partial datasets. Consequently, Fig. 3 depicts the training set loss of the global (consensus) model across different methods to compare their performance.

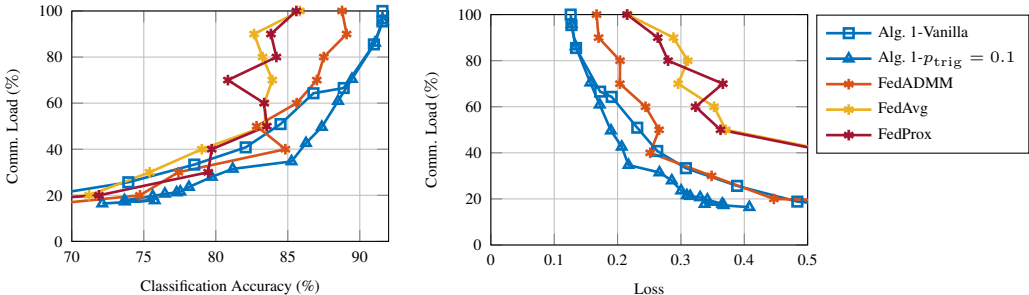


Figure 3: The figure compares different federated learning methods with respect to the resulting trade-off between total communication load and classification accuracy (left panel) and loss (right panel) on the entire dataset.

The comparison with other federated learning methods emphasizes the challenges associated with non-i.i.d. data distribution and communication overhead. FedAvg, as highlighted in [Li et al., 2020c], experiences slowdowns in the presence of non-i.i.d. data, and increasing participation does not necessarily alleviate this issue. FedProx has the same issue and is unable to converge to a classifier that generalizes across all digits. FedADMM can indeed cope with non-i.i.d. data, but has disadvantages related to the random sampling mechanism. Notably, all baselines employ a random selection of agents, which, in non-i.i.d. scenarios, misses crucial changes and results in a waste of communication resources. Our method addresses these challenges by adopting an event-based agent selection approach.

## 6 Conclusion

We introduce an event-based distributed learning approach that effectively reduces communication overhead by triggering events only when local models undergo significant changes. The method, based on over-relaxed ADMM, exhibits accelerated convergence rates in convex settings, demonstrates robustness to communication drops, and outperforms common baselines such as FedAvg, FedProx, and FedADMM in our experiments, which include an MNIST and CIFAR-10 learning task. The experiments highlight that savings of more than 50% are possible without significantly degrading the solution accuracy. The method allows for explicit trade-offs between communication load and solution accuracy, making it promising for large-scale learning systems with heterogeneous data and communication constraints.

## Acknowledgments and Disclosure of Funding

Guener Dilsad ER and Michael Muehlebach thank the German Research Foundation and the International Max Planck Research School for Intelligent Systems (IMPRS-IS) for their support. The authors also thank Michael Cummins for his contribution to the CIFAR-10 classifier.

## References

- Durmus Alp Emre Acar, Yue Zhao, Ramon Matas Navarro, Matthew Mattina, Paul N. Whatmough, and Venkatesh Saligrama. Federated learning based on dynamic regularization. *Proceedings of the International Conference on Learning Representations*, pages 1–36, 2021.
- Muhammad Asad, Saima Shaukat, Dou Hu, Zekun Wang, Ehsan Javanmardi, Jin Nakazato, and Manabu Tsukada. Limitations and future aspects of communication costs in federated learning: A survey. *Sensors*, 23(17):7358, 2023.
- Nicola Bastianello, Ruggero Carli, Luca Schenato, and Marco Todescato. Asynchronous distributed optimization over lossy networks via relaxed ADMM: Stability and linear convergence. *IEEE Transactions on Automatic Control*, 66(6):2620–2635, 2021.
- Dimitri P. Bertsekas and John N. Tsitsiklis. *Parallel and Distributed Computation: Numerical Methods*. Athena Scientific, 1989.
- Stephen Boyd, Neal Parikh, Eric Chu, Borja Peleato, and Jonathan Eckstein. Distributed optimization and statistical learning via the alternating direction method of multipliers. *Foundations and Trends in Machine Learning*, 3(1):1–122, 2010.
- Emmanuel J. Candès, Xiaodong Li, Yi Ma, and John Wright. Robust principal component analysis. *Journal of the ACM*, 58(3):1–37, 2011.
- Xuanyu Cao, Tamer Başar, Suhas Diggavi, Yonina C. Eldar, Khaled B. Letaief, H. Vincent Poor, and Junshan Zhang. Communication-efficient distributed learning: An overview. *Journal on Selected Areas in Communications*, 41(4):851–873, 2023.
- Li Deng. The MNIST database of handwritten digit images for machine learning research. *IEEE Signal Processing Magazine*, 29(6):141–142, 2012.
- Yonghai Gong, Yichuan Li, and Nikolaos M. Freris. FedADMM: A robust federated deep learning framework with adaptivity to system heterogeneity. *Proceedings of the IEEE International Conference on Data Engineering*, pages 2575–2587, 2022.
- Hadrien Hendrikx, Lin Xiao, Sébastien Bubeck, Francis Bach, and Laurent Massoulié. Statistically preconditioned accelerated gradient method for distributed optimization. *Proceedings of the International Conference on Machine Learning*, 119:4203–4227, 2020.
- Peter Kairouz et al. Advances and Open Problems in Federated Learning. *Foundations and Trends in Machine Learning*, 14(1-2):1–210, 2021.
- Dmitry Kovalev, Adil Salim, and Peter Richtárik. Optimal and practical algorithms for smooth and strongly convex decentralized optimization. *Proceedings of the Conference on Advances in Neural Information Processing Systems*, pages 18342–18352, 2020.
- Alex Krizhevsky. Learning multiple layers of features from tiny images. *Technical Report, University of Toronto*, 2009.
- Laurent Lessard, Benjamin Recht, and Andrew Packard. Analysis and design of optimization algorithms via integral quadratic constraints. *SIAM Journal on Optimization*, 26(1):57–95, 2016.
- Meng Li, Mehrdad Sanjabi, and Martin Jaggi. Federated optimization in heterogeneous networks. *Proceedings of the Conference on Machine Learning and Systems*, 2:429–450, 2020a.
- Tian Li, Anit Kumar Sahu, Ameet Talwalkar, and Virginia Smith. Federated learning: Challenges, methods, and future directions. *IEEE Signal Processing Magazine*, 37(3):50–60, 2020b.
- Xiang Li, Wenhao Yang, Kaixuan Huang, Shusen Wang, and Zhihua Zhang. On the convergence of FedAvg on non-i.i.d. *Proceedings of the International Conference on Learning Representations*, pages 1–26, 2020c.

- Yanli Liu, Yuejiao Sun, and Wotao Yin. Decentralized learning with lazy and approximate dual gradients. *IEEE Transactions on Signal Processing*, 69:1362–1377, 2021.
- Yaohua Liu, Wei Xu, Gang Wu, Zhi Tian, and Qing Ling. Communication-censored ADMM for decentralized consensus optimization. *IEEE Transactions on Signal Processing*, 67(10):2565–2579, 2019.
- H Brendan McMahan, Eider Moore, Daniel Ramage, and Seth Hampson. Communication-Efficient Learning of Deep Networks from Decentralized Data. *Proceedings of the International Conference on Artificial Intelligence and Statistics*, 54:1273–1282, 2017.
- Marek Miskowicz. Send-On-Delta Concept: An Event-Based Data Reporting Strategy. *Sensors*, 6(1):49–63, 2006.
- Michael Muehlebach and Michael I Jordan. A Dynamical Systems Perspective on Nesterov Acceleration. *Proceedings of the International Conference on Machine Learning*, 97:4656–4662, 2019.
- Michael Muehlebach and Michael I. Jordan. Continuous-time lower bounds for gradient-based algorithms. *Proceedings of the International Conference on Machine Learning*, 119:7088–7096, 2020.
- Adel Nabli and Edouard Oyallon. DADAO: Decoupled accelerated decentralized asynchronous optimization. *Proceedings of the International Conference on Machine Learning*, 202:25604–25626, 2023.
- Angelia Nedic, Alex Olshevsky, and Michael G. Rabbat. Network Topology and Communication-Computation Tradeoffs in Decentralized Optimization. *Proceedings of the IEEE*, 106(5):953–976, 2018.
- Robert Nishihara, Laurent Lessard, Benjamin Recht, Andrew Packard, and Michael I. Jordan. A general analysis of the convergence of ADMM. *Proceedings of the International Conference on Machine Learning*, 37:343–352, 2015.
- Boris T. Polyak. *Introduction to optimization*. Optimization Software Inc., Publications Division, New York, 1987.
- Amirhossein Reisizadeh, Ali Jadbabaie, Aryan Mokhtari, Hamed Hassani, and Ramtin Pedarsani. FedPAQ: A communication-efficient federated learning method with periodic averaging and quantization. *Proceedings of the International Conference on Artificial Intelligence and Statistics*, 108:2021–2031, 2020.
- Ohad Shamir, Nathan Srebro, and Tong Zhang. Communication-efficient distributed optimization using an approximate Newton-type method. *Proceedings of the International Conference on Machine Learning*, 32(2):1000–1008, 2014.
- Yong Shi, Yuanying Zhang, Peng Zhang, Yang Xiao, and Lingfeng Niu. Federated learning with  $\ell_1$  regularization. *Pattern Recognition Letters*, 172:15–21, 2023.
- Reza Shokri and Vitaly Shmatikov. Privacy-preserving deep learning. *Proceedings of the SIGSAC Conference on Computer and Communications Security*, pages 1310–1321, 2015.
- Navjot Singh, Deepesh Data, Jemin George, and Suhas Diggavi. SPARQ-SGD: Event-triggered and compressed communication in decentralized optimization. *IEEE Transactions on Automatic Control*, 68(2):721–736, 2023.
- Weijie Su, Stephen Boyd, and Emmanuel J Candes. A Differential Equation for Modeling Nesterov’s Accelerated Gradient Method: Theory and Insights. *Journal of Machine Learning Research*, 17(153):1–43, 2016.
- Guanchun Tong and Michael Muehlebach. A dynamical systems perspective on discrete optimization. *Proceedings of Machine Learning Research*, 211:1–14, 2023.
- Han Wang, Siddhartha Marella, and James Anderson. FedADMM: A federated primal-dual algorithm allowing partial participation. *Proceedings of the IEEE Conference on Decision and Control*, pages 287–294, 2022.
- Ermin Wei and Asuman Ozdaglar. Distributed alternating direction method of multipliers. *Proceedings of the IEEE Conference on Decision and Control*, pages 5445–5450, 2012.
- Wei Liu, Li Chen, and Wenyi Zhang. Decentralized Federated Learning: Balancing Communication and Computing Costs. *IEEE Transactions on Signal and Information Processing over Networks*, 8:131–143, 2021.
- Andre Wibisono, Ashia C. Wilson, and Michael I Jordan. A variational perspective on accelerated methods in optimization. *Proceedings of the National Academy of Sciences*, 113(47):E7351–E7358, 2016.

- Ziyi Yu and Nikolaos M. Freris. Communication-efficient distributed optimization with adaptability to system heterogeneity. *Proceedings of the IEEE Conference on Decision and Control*, pages 3321–3326, 2023.
- Xinwei Zhang, Mingyi Hong, Sairaj Dhople, Wotao Yin, and Yang Liu. FedPD: A federated learning framework with adaptivity to non-iid data. *IEEE Transactions on Signal Processing*, 69:6055–6070, 2021.
- Zhen Zhang, Shaofu Yang, and Wenying Xu. Decentralized ADMM with compressed and event-triggered communication. *Neural Networks*, 165:472–482, 2023.
- Zhen Zhang, Shaofu Yang, Wenying Xu, and Kai Di. Privacy-preserving distributed ADMM with event-triggered communication. *IEEE Transactions on Neural Networks and Learning Systems*, 35(2):2835–2847, 2024.
- Yue Zhao, Meng Li, Liangzhen Lai, Naveen Suda, Damon Civin, and Vikas Chandra. Federated learning with non-iid data. *arxiv:1806.00582*, 2018.
- Shenglong Zhou and Geoffrey Ye Li. Federated learning via inexact ADMM. *IEEE Transactions on Pattern Analysis and Machine Intelligence*, 45(8):9699–9708, 2023.

## A Communication Structure

This section discusses the sharing problem and consensus reaching over graphs as two special cases of the more general constrained minimization problem formulation

$$\min_{x \in \mathbb{R}^p, z \in \mathbb{R}^q} f(x) + g(z), \quad \text{subject to } Ax + Bz = c, \quad (4)$$

with variables  $x \in \mathbb{R}^p$  and  $z \in \mathbb{R}^q$  and constant matrices  $A \in \mathbb{R}^{r \times p}$ ,  $B \in \mathbb{R}^{r \times q}$ , and  $c \in \mathbb{R}^r$ . The objective function is decomposed into a smooth part  $f : \mathbb{R}^p \rightarrow \mathbb{R}$  and nonsmooth part  $g : \mathbb{R}^q \rightarrow \mathbb{R}$ . The communication structure of the problem formulation (4) is shown in Fig. 4, where primal, dual and auxiliary variables are treated as different communication nodes.

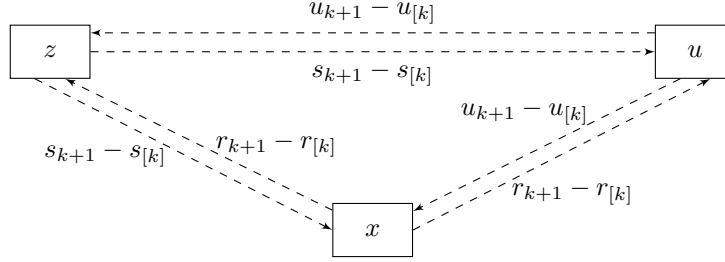


Figure 4: The communication structure that arises from Alg. 2, where  $s := Bz$ ,  $r := Ax$ , and  $u$  denotes the dual variable.

### A.1 Sharing Problem

We will show that the event-based communication structure introduced in Fig. 4 simplifies considerably for the sharing problem. The sharing problem takes the following form,

$$\min_{x^1, \dots, x^N \in \mathbb{R}^p} \sum_{i=1}^N f^i(x^i) + g\left(\sum_{i=1}^N x^i\right),$$

and arises as a special case from (4) when choosing  $f(x) = \sum_{i=1}^N f^i(x^i)$ ,  $x = (x^1, x^2, \dots, x^N) \in \mathbb{R}^{Np}$ ,  $A = I_{Np}$ ,  $B = -(I_p, I_p, \dots, I_p)$ ,  $c = 0$ . The problem can be solved via the following updates, by agents  $i = 1, \dots, N$ ;

$$x_{k+1}^i = \operatorname{argmin}_{x^i \in \mathbb{R}^p} f^i(x^i) + \frac{\rho}{2} \left| x^i - x_k^i + \hat{h}_k \right|^2, \quad (5)$$

and by agent  $N + 1$ ;

$$\begin{aligned} \bar{x}_{k+1} &= \frac{1}{N} \sum_{i=1}^N \hat{x}_{k+1}^i \\ z^{k+1} &= \operatorname{argmin}_{z \in \mathbb{R}^p} g(Nz) + \frac{N\rho}{2} \left| z - \bar{x}_{k+1} - \frac{1}{\rho} u^k \right|^2 \\ u_{k+1} &= u_k + \rho (\bar{x}_{k+1} - z_{k+1}) \\ h_{k+1} &= \bar{x}_{k+1} - z_{k+1} + \frac{1}{\rho} u_{k+1}. \end{aligned} \quad (6)$$

For the sharing problem, the general communication scheme in Fig. 4 reduces to the diagram in Fig. 5, where each node communicates their local variable in an event-based manner.

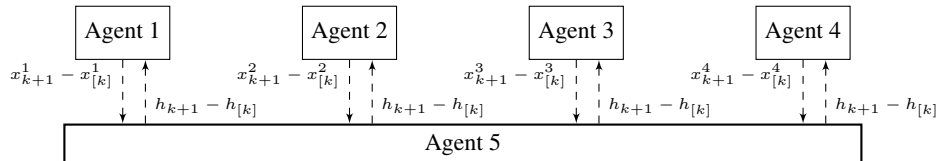


Figure 5: The diagram visualizes the communication structure for the sharing problem for  $N = 4$  agents.

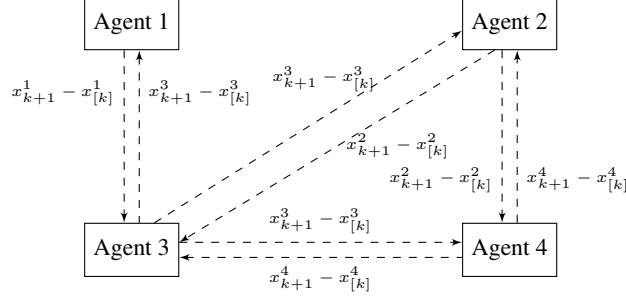


Figure 6: The diagram visualizes the communication structure for a distributed learning problem over a graph that connects four agents with four edges.

## A.2 Consensus over a Graph

As another example, we will show that (4) also generalizes to distributed learning scenarios over graphs. We consider a network topology, captured by an undirected connected graph  $\mathcal{G} = (\mathcal{V}, \mathcal{E})$ , where  $\mathcal{V} = \{1, \dots, N\}$  is the set of vertices and  $\mathcal{E} \subseteq \mathcal{V} \times \mathcal{V}$  is the set of edges. Each agent (vertex) has a local data distribution, and the aim is to train a model without a central server to aggregate the collected information. The problem can be formulated as follows:

$$\min_{x^i \in \mathbb{R}^p, z^{ij} \in \mathbb{R}^p} \sum_{i=1}^N f^i(x^i), \quad \text{subject to } x^i = z^{ij}, x^j = z^{ij}, \quad \forall (i, j) \in \mathcal{E}.$$

Similar to the formulation in [Yu and Freris, 2023], we define transmitter and receiver matrices  $\hat{A}_t, \hat{A}_r \in \mathbb{R}^{|\mathcal{E}| \times N}$  for all edges, i.e.,

$$\left[ \hat{A}_t \right]_{ei} = \left[ \hat{A}_r \right]_{ej} = \begin{cases} 1 & (i, j) \in \mathcal{E} \\ 0 & \text{otherwise} \end{cases}, \quad \forall e \in \mathcal{E}.$$

By stacking  $x^i, z^{ij} \in \mathbb{R}^p$  into column vectors  $x \in \mathbb{R}^{Np}, z \in \mathbb{R}^{|\mathcal{E}|p}$ , respectively, we conclude that distributed learning over graphs is indeed a special case of (4),

$$\min_{x \in \mathbb{R}^{Np}, z \in \mathbb{R}^{|\mathcal{E}|p}} f(x), \quad \text{subject to } \begin{bmatrix} \hat{A}_t \otimes I_p \\ \hat{A}_r \otimes I_p \end{bmatrix} x = \begin{bmatrix} I_{|\mathcal{E}|p} \\ I_{|\mathcal{E}|p} \end{bmatrix} z,$$

where  $\otimes$  denotes the Kronecker product and  $I_p$  the identity matrix. Thus, the matrices  $A$  and  $B$  encode the topology of the communication graph, which will affect the convergence rates as highlighted with our main result Thm. 4.1 where the convergence rate is dictated by the value  $\kappa = \bar{\sigma}(A)L/(\underline{\sigma}(A)m)$ .

The resulting instance of Alg. 1 takes the following form:

$$\begin{aligned} x_{k+1}^i &= \operatorname{argmin}_{x^i \in \mathbb{R}^p} f_i(x^i) + \frac{|\mathcal{N}_i| \rho}{2} \left| x^i - \frac{1}{2} (x_i^k - \bar{x}_k^i) + \frac{1}{\rho} p_k^i \right|^2 \\ \bar{x}_{k+1}^i &= \frac{1}{|\mathcal{N}_i|} \sum_{j \in \mathcal{N}_i} \hat{x}_{k+1}^j \\ p_{k+1}^i &= p_k^i + \frac{\rho}{2} (x_{k+1}^i - \bar{x}_{k+1}^i), \end{aligned} \tag{7}$$

where  $\mathcal{N}_i$  represents the set containing the neighbors of the agent  $i$  and  $|\mathcal{N}_i|$  is the number of vertices. In the event based-communication setting, an agent transmits its local model ( $x_{k+1}^i$ ) to the neighbors only if there has been a significant change in the local model. Fig. 6 shows an example with four agents, each communicating local variables only.

## B Derivation of Alg. 2 as a Dynamical System

In this section, we represent Alg. 2 as a dynamical system that consists of linear dynamics with a nonlinear feedback interconnection. The communication structure is summarized with Fig. 2.

For the convenience of the reader, we start by restating Alg. 2, which is based on an over-relaxed ADMM algorithm.

---

### Algorithm 3 Event-Based Distributed Optimization with Over-Relaxed ADMM

---

**Require:** Functions  $f$  and  $g$ , matrices  $A$  and  $B$ , vector  $c$ , parameters  $\rho$  and  $\alpha$

**Require:** Initial condition  $x_0, z_0$

$$r_0 = \hat{r}_0^s = \hat{r}_0^u = Ax_0, \quad s_0 = \hat{s}_0^r = \hat{s}_0^u = Bz_0, \quad u_0 = \hat{u}_0^r = \hat{u}_0^s = 0$$

**for**  $k = 0$  to  $t_{\max}$  **do**

$$\hat{s}_k^r, \hat{u}_k^r \leftarrow \text{event-based receive of } s_{k+1} - s_{[k]}, u_{k+1} - u_{[k]}$$

$$x_{k+1} = \arg \min_x f(x) + \frac{\rho}{2} |Ax + \hat{s}_k^r - c + \hat{u}_k^r|^2 \quad \{\text{r-agent}\}$$

$$\text{event-based send of } r_{k+1} - r_{[k]} \text{ where } r_{k+1} = Ax_{k+1}$$

$$\hat{r}_{k+1}^s, \hat{u}_k^s \leftarrow \text{event-based receive of } r_{k+1} - r_{[k]}, u_{k+1} - u_{[k]}$$

$$z_{k+1} = \arg \min_z g(z) + \frac{\rho}{2} |\alpha \hat{r}_{k+1}^s - (1 - \alpha)Bz_k + Bz - \alpha c + \hat{u}_k^s|^2 \quad \{\text{s-agent}\}$$

$$\text{event-based send of } s_{k+1} - s_{[k]} \text{ where } s_{k+1} = Bz_{k+1}$$

$$\hat{r}_{k+1}^u, \hat{s}_{k+1}^u \leftarrow \text{event-based receive of } r_{k+1} - r_{[k]}, s_{k+1} - s_{[k]}$$

$$u_{k+1} = u_k + \alpha \hat{r}_{k+1}^u - (1 - \alpha) \hat{s}_k^u + \hat{s}_{k+1}^u - \alpha c \quad \{\text{u-agent}\}$$

$$\text{event-based send of } u_{k+1} - u_{[k]}$$

**if**  $\text{mod}(k + 1, T) = 0$  **then**

$$\text{reset} \rightarrow \hat{r}_{k+1}^{u;s} = r_{k+1}, \hat{s}_{k+1}^{u;r} = s_{k+1}, u_{k+1}^{r;s} = u_{k+1}$$

**end if**

**end for**

---

The following definitions will be useful for simplifying the updates of the iterates:

**Definition 1.** Let Assmp. 1 and 2 hold. We define the function  $\hat{f} : \mathbb{R}^n \rightarrow \mathbb{R}$  as follows,

$$\hat{f} = (\rho^{-1}f) \circ A^{-1}, \quad (8)$$

where  $\rho$  is the step-size of Alg. 2. The function is  $\hat{m} := m/(\rho\bar{\sigma}^2(A))$ -strongly convex and  $\hat{L} := L/(\rho\bar{\sigma}^2(A))$ -smooth, and has therefore the condition number

$$\kappa := \frac{\hat{L}}{\hat{m}} = \frac{L}{m} \frac{\bar{\sigma}^2(A)}{\bar{\sigma}^2(A)}.$$

**Definition 2.** Let Assmp. 1 and 2 hold. The function  $\hat{g} : \mathbb{R}^m \rightarrow \bar{\mathbb{R}}$  is defined as

$$\hat{g} = (\rho^{-1}g) \circ B^\dagger + \psi_{\text{im}(B)}, \quad (9)$$

where  $B^\dagger$  is the Moore-Penrose inverse of  $B$ ,  $\psi_{\text{im}(B)}$  is the indicator function of the image of  $B$ , and  $\rho$  is the step-size of Alg. 2.

We proceed by summarizing the notation that will be used subsequently. The sequences  $r_k$  and  $s_k$  are defined as  $r_k := Ax_k$  and  $s_k := Bz_k$ . We introduced the variable  $\hat{r}_k^s$ , for example, which models agent  $s$ 's estimate of the variable  $r_k$ . The variables  $\hat{r}_k^u, \hat{s}_k^r, \hat{s}_k^u$ , etc., are defined analogously and follow the notational convention

$$\widehat{\text{variable}}_{\text{receiving\_agent } k} := \text{receiving\_agent's estimate of variable at time } k.$$

As a result of the event-based communication, the local estimates  $\hat{r}_k^s, \hat{r}_k^u, \hat{s}_k^r$ , etc., differ from  $r_k, s_k$ , etc. These differences will be captured by the variable  $\varepsilon$  for which we introduce the following notational convention:

$$\begin{aligned} \varepsilon_k^{\text{variable, receiving\_agent}} &:= \widehat{\text{variable}}_{\text{receiving\_agent } k} - \text{variable}_k \\ &= \text{receiving\_agent's estimation error of variable at time } k. \end{aligned}$$

We further introduce the error

$$e_k := (\varepsilon_{k+1}^{rs}, \varepsilon_{k+1}^{ru}, \varepsilon_{k+1}^{su}, \varepsilon_k^{sr}, \varepsilon_k^{su}, \varepsilon_k^{ur}, \varepsilon_k^{us}), \quad (10)$$

that collects the estimation errors of the different agents. By virtue of the event-based communication mechanism and the reset mechanism, the error  $e_k$  is bounded by the communication threshold  $\Delta$ . We finally introduce the notation for the corresponding communication thresholds,  $\Delta^{rs}$ ,  $\Delta^{sr}$ , etc. (see Fig. 2), according to the same rationale:

$\Delta^{\text{variable, receiving\_agent}}$  := threshold for triggering a communication of variable to receiving\\_agent.

To sum up, the vector  $e_k$  contains the errors on the communication lines shown on Fig. 2. For example,  $\varepsilon_{k+1}^{rs}$  stands for the difference between the actual value of state  $r_{k+1}$  and agent  $s$ 's estimate  $\hat{r}_{k+1}^s$ , that is,  $\varepsilon_{k+1}^{rs} = \hat{r}_{k+1}^s - r_{k+1}$  at time step  $k + 1$ .

If the value  $r_{k+1}$  has deviated more than  $\Delta^{rs}$  amount since the time-step  $[k]$ , where the last value  $r_{[k]}$  has been communicated to the agent  $s$ , a communication is triggered. This means  $rs \in \mathcal{C}_{k+1}$ .

$$|r_{k+1} - r_{l_k}^{rs}| > \Delta^{rs} \iff rs \in \mathcal{C}_{k+1} \iff [k+1] = k+1.$$

The set  $\mathcal{D}_{k+1}$ , which is a subset of  $\mathcal{C}_{k+1}$ , collects indices of failed transmission lines at time step  $k + 1$ . We further introduce that the superscript  $c$  to denote the complement of a set. If the communication does not fail, that is,  $rs \in \mathcal{D}_{k+1}^c$ , then agent  $s$ 's estimate of  $r_{k+1}$  is updated as follows.

$$rs \in \mathcal{C}_{k+1} \wedge rs \in \mathcal{D}_{k+1}^c \iff \hat{r}_{k+1}^s = \hat{r}_k^s + (r_{k+1} - r_{[k]}).$$

To incorporate the effect of communication drops, we introduce the variable  $\chi_{k+1}^{rs}$ , which represents the disturbance that results from dropped communications,

$$rs \in \mathcal{D}_{k+1} \Rightarrow \chi_{k+1}^{rs} = -(r_{k+1} - r_{[k]}). \quad (11)$$

Therefore, the dynamics of  $\hat{r}_{k+1}^s$  are expressed as follows

$$\hat{r}_{k+1}^s = r_{[k+1]} + \sum_{l=1}^{k+1} \chi_l^{rs}. \quad (12)$$

When deriving the previous equation, we have exploited the fact that

$$\begin{aligned} rs \in \mathcal{C}_{k+1} &\Rightarrow [k+1] = k+1 \\ rs \in \mathcal{C}_{k+1}^c &\Rightarrow [k+1] = [k]. \end{aligned}$$

To summarize, in the case of communication drop, the agent  $s$  updates the image of  $r$  with a disturbed value.

We now express the different minimization steps in Alg. 3 by their corresponding stationarity conditions, and simplify the corresponding expressions. The minimization step for the primal variable  $x$  can be rewritten as follows

$$\begin{aligned} x_{k+1} &= \arg \min_{x \in \mathbb{R}^p} f(x) + \frac{\rho}{2} |Ax + \hat{s}_k^r - c + \hat{u}_k^r|^2 \\ &= A^{-1} \arg \min_{r \in \mathbb{R}^n} f(A^{-1}r) + \frac{\rho}{2} |r + \hat{s}_k^r - c + \hat{u}_k^r|^2, \end{aligned}$$

due to the fact that  $A$  is invertible, which yields

$$r_{k+1} = \arg \min_{r \in \mathbb{R}^n} \hat{f}(r) + \frac{1}{2} |r + \hat{s}_k^r - c + \hat{u}_k^r|^2.$$

The variable  $r_{k+1}$  satisfies therefore the following stationarity condition

$$0 = \nabla \hat{f}(r_{k+1}) + r_{k+1} + \hat{s}_k^r - c + \hat{u}_k^r,$$

which can be rearranged to

$$r_{k+1} - c = -\nabla \hat{f}(r_{k+1}) - s_k - \varepsilon_k^{sr} - u_k - \varepsilon_k^{ur}, \quad (13)$$

where  $\hat{s}_k^r$  is replaced by  $s_k + \varepsilon_k^{sr}$  and  $\hat{u}_k^r$  by  $u_k + \varepsilon_k^{ur}$ .



Similarly, the update step of the auxiliary variable  $z$  can be reformulated as

$$\begin{aligned} z_{k+1} &= \arg \min_{z \in \mathbb{R}^n} g(z) + \frac{\rho}{2} |\alpha \hat{r}_{k+1}^s - (1 - \alpha) s_k + Bz - \alpha c + \hat{u}_k^s|^2 \\ &= B^\dagger \arg \min_{s \in \mathbb{R}^m} g(B^\dagger s) + \psi_{\text{im}(B)}(s) + \frac{\rho}{2} |\alpha \hat{r}_{k+1}^s - (1 - \alpha) s_k + s - \alpha c + \hat{u}_k^s|^2, \end{aligned}$$

since the matrix  $B$  has full column rank and therefore possesses the left inverse  $B^\dagger$ . This yields

$$s_{k+1} = \arg \min_{s \in \mathbb{R}^m} \hat{g}(s) + \frac{1}{2} |\alpha \hat{r}_{k+1}^s - (1 - \alpha) s_k + s - \alpha c + \hat{u}_k^s|^2,$$

and implies the following stationarity condition for  $s_{k+1}$

$$0 \in \partial \hat{g}(s_{k+1}) + \alpha \hat{r}_{k+1}^s - (1 - \alpha) s_k + s_{k+1} - \alpha c + \hat{u}_k^s. \quad (14)$$

This stationarity condition can be reformulated as

$$s_{k+1} = s_k + (\alpha - 1) u_k + \alpha \nabla \hat{f}(r_{k+1}) - \gamma_{k+1} - \varepsilon_k^{us} + \alpha \varepsilon_k^{sr} + \alpha \varepsilon_k^{ur} - \alpha \varepsilon_{k+1}^{rs}, \quad (15)$$

for some  $\gamma_{k+1} \in \partial \hat{g}(s_{k+1})$ , and where we have expressed  $\hat{r}_{k+1}^s$  as  $r_{k+1} + \varepsilon_{k+1}^{rs}$  and  $\hat{u}_k^s$  as  $u_k + \varepsilon_k^{us}$ . We have further replaced  $r_{k+1} - c$  by the expression given in (13).

The update of the dual variables  $u_k$  evolve according to the following dynamics:

$$\begin{aligned} u_{k+1} &= u_k + \alpha \hat{r}_{k+1}^u - (1 - \alpha) \hat{s}_k^u + \hat{s}_{k+1}^u - \alpha c \\ &= u_k + \alpha (r_{k+1} + \varepsilon_{k+1}^{ru}) - (1 - \alpha) (s_k + \varepsilon_k^{su}) + (s_{k+1} + \varepsilon_{k+1}^{su}) - \alpha c. \end{aligned}$$

The dynamics can be further simplified by replacing  $s_{k+1}$  with the help of (14), which yields:

$$u_{k+1} = -\gamma_{k+1} - \alpha \varepsilon_{k+1}^{rs} + \alpha \varepsilon_{k+1}^{ru} + \varepsilon_{k+1}^{su} + (\alpha - 1) \varepsilon_k^{su} - \varepsilon_k^{us}. \quad (16)$$

As a result of these simplifications, we note that  $r_{k+1}$  is uniquely determined by  $s_k$ ,  $u_k$  and the corresponding errors  $\varepsilon_k^{sr}$  and  $\varepsilon_k^{ur}$ . We further note that according to (15) and (16) the iterates of Alg. 3 can be represented as an interconnection between a linear dynamical system, with a nonlinear feedback interconnection that models the evaluation of the gradient  $\nabla \hat{f}$  and  $\partial \hat{g}$ . The state of the dynamical system is therefore chosen as  $\xi_k := (s_k, u_k)$ , the output as  $y_k := (r_{k+1} - c, s_{k+1})$ , and the input as  $v_k := (\nabla \hat{f}(r_{k+1}), \gamma_{k+1})$ , where  $\gamma_{k+1} \in \partial \hat{g}(s_{k+1})$ . We also define output variables  $w_k^1 := (r_{k+1} - c, \nabla \hat{f}(r_{k+1}))$ ,  $w_k^2 := (s_{k+1}, \gamma_{k+1})$ , which will be employed for the convergence analysis.

According to these definitions, we can express the iterates of Alg. 3 as trajectories of the following nonlinear dynamical system,

$$\xi_{k+1} = \underbrace{\begin{bmatrix} 1 & \alpha - 1 \\ 0 & 0 \end{bmatrix}}_{:=\hat{A}} \xi_k + \underbrace{\begin{bmatrix} \alpha & -1 \\ 0 & -1 \end{bmatrix}}_{:=\hat{B}} v_k + \underbrace{\begin{bmatrix} -\alpha & 0 & 0 & \alpha & 0 & \alpha & -1 \\ -\alpha & \alpha & 1 & 0 & \alpha & -1 & 0 & -1 \end{bmatrix}}_{:=\hat{E}} e_k, \quad v_k = \phi(y_k), \quad (17)$$

$$y_k = \underbrace{\begin{bmatrix} -1 & -1 \\ 1 & \alpha - 1 \end{bmatrix}}_{:=\hat{C}} \xi_k + \underbrace{\begin{bmatrix} -1 & 0 \\ \alpha & -1 \end{bmatrix}}_{:=\hat{D}} v_k + \underbrace{\begin{bmatrix} 0 & 0 & 0 & -1 & 0 & -1 & 0 \\ -\alpha & 0 & 0 & \alpha & 0 & \alpha & -1 \end{bmatrix}}_{:=\hat{E}^y} e_k,$$

$$w_k^1 = \underbrace{\begin{bmatrix} -1 & -1 \\ 0 & 0 \end{bmatrix}}_{:=\hat{C}^1} \xi_k + \underbrace{\begin{bmatrix} -1 & 0 \\ 1 & 0 \end{bmatrix}}_{:=\hat{D}^1} v_k + \underbrace{\begin{bmatrix} 0 & 0 & 0 & -1 & 0 & -1 & 0 \\ 0 & 0 & 0 & 0 & 0 & 0 & 0 \end{bmatrix}}_{:=\hat{E}^1} e_k,$$

$$w_k^2 = \underbrace{\begin{bmatrix} 1 & \alpha - 1 \\ 0 & 0 \end{bmatrix}}_{:=\hat{C}^2} \xi_k + \underbrace{\begin{bmatrix} \alpha & -1 \\ 0 & 1 \end{bmatrix}}_{:=\hat{D}^2} v_k + \underbrace{\begin{bmatrix} -\alpha & 0 & 0 & \alpha & 0 & \alpha & -1 \\ 0 & 0 & 0 & 0 & 0 & 0 & 0 \end{bmatrix}}_{:=\hat{E}^2} e_k, \quad (18)$$

where  $\phi$  denotes the nonlinear feedback interconnection that captures the evaluation of the gradients  $\nabla \hat{f}$  and  $\partial \hat{g}$ . Fig. 7 provides a graphical representation of the time-invariant dynamics determined by the matrices  $\hat{A}, \hat{B}, \hat{C}, \hat{D}$ .

We close the section with the following proposition that shows that  $|e_k|$  is bounded.

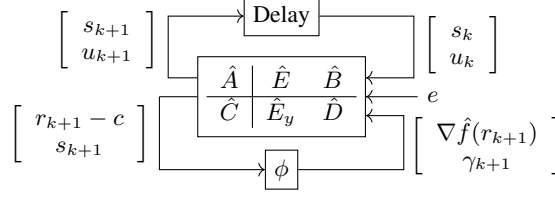


Figure 7: The dynamical system following (17) is visualized.

**Proposition B.1.** *The error  $e_k$  at iteration  $k$  is bounded by*

$$|e_k| \leq \Delta, \quad \Delta := \sum_{l \in \{rs, ru, sr, su, ur, us\}} \Delta^l + T\bar{\chi}^l,$$

where the variable  $\bar{\chi}^l$  is an upper bound on the communication drops.

*Proof.* The proof is analogous to Prop. 2.1. The error resulting from the event-based communication structure is given by

$$\varepsilon_{k+1}^{rs} = \hat{r}_{k+1}^s - r_{k+1} = \underbrace{r_{[k+1]} - r_{k+1}}_I + \underbrace{\sum_{l=1}^{k+1} \chi_l^{rs}}_{II}. \quad (19)$$

We further note that the first term is bounded by  $\Delta^{rs}$  by virtue of the communication rule

$$|r_{k+1} - r_{[k+1]}| \leq \Delta^{rs}.$$

Through the assumption  $|\chi_l^{rs}| \leq \bar{\chi}^{rs}$ , the second part is bounded by  $T\bar{\chi}^{rs}$ , where  $T$  is the reset period. Therefore, we conclude that  $|e_{k+1}^{rs}|$  is bounded by  $\Delta^{rs} + T\bar{\chi}^{rs}$ . Similarly, the other elements of the vector  $e_k$  are bounded by  $\Delta^{ru} + T\bar{\chi}^{ru}$ ,  $\Delta^{su} + T\bar{\chi}^{su}$ , etc. Hence,  $|e_k|$  is bounded by  $\Delta$  where

$$\Delta = \sum_{l \in \{rs, ru, sr, su, ur, us\}} \Delta^l + T\bar{\chi}^l.$$

□

The analysis indicates that a periodic reset with a period  $T$  is required to achieve a bounded error. If no reset is included, Alg. 2 may not converge, which could result in a large error that accumulates over time. The dependence of  $\Delta$  on the period  $T$  highlights how the reset period  $T$  affects the error (where smaller  $T$  leads to a smaller error bound). If there are no communication failures, there is also no need for a reset ( $\bar{\chi} = 0$ ), and  $\Delta$  reduces to the collection of communication thresholds.

## C Convergence Analysis

We first start by proving the following intermediate lemmas.

**Lemma C.1.** *Let Assmp. 2 be satisfied. Then, the following holds,*

$$[(r_1 - r_2)^\top (\nabla \hat{f}(r_1) - \nabla \hat{f}(r_2))^\top] \left( \begin{bmatrix} -2\hat{m}\hat{L} & (\hat{m} + \hat{L}) \\ (\hat{m} + \hat{L}) & -2 \end{bmatrix} \otimes I_n \right) \begin{bmatrix} r_1 - r_2 \\ \nabla \hat{f}(r_1) - \nabla \hat{f}(r_2) \end{bmatrix} \geq 0, \quad (20)$$

for all  $r_1, r_2 \in \mathbb{R}^n$ .

*Proof.* We define the auxiliary function  $\tilde{f}(r) := \hat{f}(r) - \frac{\hat{m}}{2}|r|^2$ , which is  $\hat{L} - \hat{m}$ -smooth and convex by the properties of  $\hat{f}$ . Then the following inequality holds,

$$(\nabla \tilde{f}(r_1) - \nabla \tilde{f}(r_2))^\top (r_1 - r_2) \geq \frac{1}{\hat{L} - \hat{m}} |\nabla \tilde{f}(r_1) - \nabla \tilde{f}(r_2)|^2,$$

for any  $r_1, r_2 \in \mathbb{R}^n$ . Substituting  $\tilde{f}(r) := \hat{f}(r) - \frac{\hat{m}}{2}|r|^2$  and  $\nabla \tilde{f}(r) = \nabla \hat{f}(r) - \hat{m}r$ , we get

$$(\hat{m} + \hat{L})(r_1 - r_2)^\top (\nabla \hat{f}(r_1) - \nabla \hat{f}(r_2)) \geq \hat{m}\hat{L}|r_1 - r_2|^2 + |\nabla \hat{f}(r_1) - \nabla \hat{f}(r_2)|^2,$$

which yields the desired result.  $\square$

**Lemma C.2.** *Let Assmp. 2 be satisfied. Then, the following holds,*

$$[(s_1 - s_2)^\top (\gamma_1 - \gamma_2)^\top] \left( \begin{bmatrix} 0 & 1 \\ 1 & 0 \end{bmatrix} \otimes I_m \right) \begin{bmatrix} s_1 - s_2 \\ \gamma_1 - \gamma_2 \end{bmatrix} \geq 0, \quad (21)$$

where  $\gamma_1 \in \partial \hat{g}(s_1)$  and  $\gamma_2 \in \partial \hat{g}(s_2)$  and for any  $s_1, s_2 \in \mathbb{R}^m$ .

*Proof.* The subdifferential of a convex function is a monotone operator, and therefore

$$(s_1 - s_2)^\top (\gamma_1 - \gamma_2) \geq 0.$$

$\square$

**Lemma C.3.** *Let  $x_*, z_*$  denote the minimizer of (2) and define  $r_* := Ax_*$ ,  $s_* := Bz_*$ ,  $\beta_* := \nabla \hat{f}(r_*)$ , and  $\gamma_* \in \partial \hat{g}(s_*)$ . Then, the iterates of Alg. 3 with step-size  $\rho = \rho_0(\hat{m}\hat{L})^{\frac{1}{2}}$  satisfy*

$$(w_k^i - w_*^i)^\top M^i (w_k^i - w_*^i) \geq 0, \quad \forall i \in \{1, 2\}, \quad \forall k \geq 0,$$

with

$$M^1 := \begin{bmatrix} -2\rho_0^{-2} & \rho_0^{-1}(\kappa^{-\frac{1}{2}} + \kappa^{\frac{1}{2}}) \\ \rho_0^{-1}(\kappa^{-\frac{1}{2}} + \kappa^{\frac{1}{2}}) & -2 \end{bmatrix} \otimes I_n, \quad M^2 := \begin{bmatrix} 0 & 1 \\ 1 & 0 \end{bmatrix} \otimes I_m,$$

where

$$w_k^1 := \begin{bmatrix} r_{k+1} - c \\ \beta_{k+1} \end{bmatrix}, \quad w_k^2 := \begin{bmatrix} s_{k+1} \\ \gamma_{k+1} \end{bmatrix}, \quad w_*^1 := \begin{bmatrix} r_* - c \\ \beta_* \end{bmatrix}, \quad w_*^2 := \begin{bmatrix} s_* \\ \gamma_* \end{bmatrix}.$$

*Proof.* The proof follows directly from Lemma C.1 and Lemma C.2.  $\square$

**Lemma C.4.** *Let the sequence  $V_k \geq 0$  satisfy*

$$V_{k+1} \leq V_k(1 - \tilde{\alpha}) + \tilde{\beta}\tilde{\alpha}, \quad (22)$$

for all  $k \geq 0$ , where the parameters  $\tilde{\alpha}, \tilde{\beta}$  satisfy  $0 < \tilde{\alpha} < 1$  and  $0 \leq \tilde{\beta}$ . Then, the following holds for all  $k \geq 0$ :

$$V_k \leq V_0(1 - \tilde{\alpha})^k + \tilde{\beta}. \quad (23)$$

*Proof.* We prove the lemma by induction.

The claim holds for  $k = 0$ . We therefore assume that the claim holds for  $k$  and show that, as a result, the claim holds for  $k + 1$ . More precisely,

$$\begin{aligned} V_{k+1} &\leq V_k(1 - \tilde{\alpha}) + \tilde{\beta}\tilde{\alpha} \\ &\leq V_0(1 - \tilde{\alpha})^{k+1} + (1 - \tilde{\alpha})\tilde{\beta} + \tilde{\beta}\tilde{\alpha} \\ &\leq V_0(1 - \tilde{\alpha})^{k+1} + \tilde{\beta}, \end{aligned} \quad (24)$$

which completes the induction argument.  $\square$

In App. B, we expressed the iterates of Alg. 3 as the trajectories of a dynamical system. The dynamical system was given as a linear time-invariant system that was interconnected in feedback with a nonlinear function  $\phi$ . We now arrive at the main result that will be used to show convergence of Alg. 3.

**Theorem C.5.** *Let Assmp. 2 be satisfied, let the step-size for Alg. 3 be  $\rho = \rho_0(\hat{m}\hat{L})^{\frac{1}{2}}$ , and let  $\xi_* = (Bz_*, u_*)$ , where  $(x_*, z_*)$  is the minimizer of (2) and  $u_*$  the corresponding dual variable.*

*Suppose there exists a positive definite matrix  $P \succ 0$ ,  $0 < \tau < 1$ , and nonnegative constants  $\lambda^1, \lambda^2, \gamma^1, \gamma^2, \gamma^3$  and  $\gamma^4$  such that the following linear matrix inequality*

$$0 \succeq \begin{bmatrix} (1+\gamma^1)\hat{A}^\top P \hat{A} - \tau^2 P & \hat{A}^\top P \hat{B} \\ \hat{B}^\top P \hat{A} & (1+\gamma^2)\hat{B}^\top P \hat{B} \end{bmatrix} + \begin{bmatrix} \hat{C}^1 & \hat{D}^1 \\ \hat{C}^2 & \hat{D}^2 \end{bmatrix}^\top \begin{bmatrix} \Lambda^1 M^1 & 0 \\ 0 & \Lambda^2 M^2 \end{bmatrix} \begin{bmatrix} \hat{C}^1 & \hat{D}^1 \\ \hat{C}^2 & \hat{D}^2 \end{bmatrix} \quad (25)$$

is satisfied, where  $\Lambda^1 = \lambda^1(1 + \gamma^3)$ ,  $\Lambda^2 = \lambda^2(1 + \gamma^4)$ . Then, for all  $k \geq 0$ , we have

$$|\xi_k - \xi_*|^2 \leq \kappa_P |\xi_0 - \xi_*|^2 \tau^{2k} + \frac{\bar{\sigma}(Q)\Delta^2}{\underline{\sigma}(P)(1 - \tau^2)}, \quad (26)$$

where  $\kappa_P = \bar{\sigma}(P)/\underline{\sigma}(P)$  denotes the condition number of the matrix  $P$ ,  $\Delta$  is a bound on the error  $e_k$  (see Prop. B.1), and

$$Q = \left(1 + \frac{1}{\gamma^1} + \frac{1}{\gamma^2}\right) \hat{E}^\top P \hat{E} + \left(1 + \frac{1}{\gamma^3} + \frac{1}{\gamma^4}\right) \sum_{i=1}^2 \lambda^i \hat{E}^{i\top} M^i \hat{E}^i. \quad (27)$$

*Proof.* We consider the following quadratic storage function,

$$V_k = (\xi_k - \xi_*)^\top P (\xi_k - \xi_*),$$

and claim that the following inequality holds for the iterates of Alg. 3:

$$\begin{aligned} V_{k+1} - \tau^2 V_k + \sum_{i=1}^2 \lambda^i (w^i - w_*^i)^\top M^i (w^i - w_*^i) &\leq \\ e_k^\top \left( \left(1 + \frac{1}{\gamma^1} + \frac{1}{\gamma^2}\right) E^\top P E + \sum_{i=1}^2 \lambda^i \left(1 + \frac{1}{\gamma^3} + \frac{1}{\gamma^4}\right) E^{i\top} M^i E^i \right) e_k. \end{aligned}$$

*Proof of the claim:* We insert the system dynamics stated in App. B into the expression on the left-hand side, which yields

$$\begin{aligned}
& V_{k+1} - \tau^2 V_k + \sum_{i=1}^2 \lambda^i (w_k^i - w_\star^i)^\top M^i (w_k^i - w_\star^i) \\
&= (\xi_{k+1} - \xi_\star)^\top P (\xi_{k+1} - \xi_\star) - \tau^2 (\xi_k - \xi_\star)^\top P (\xi_k - \xi_\star) + \sum_{i=1}^2 \lambda^i (w_k^i - w_\star^i)^\top M^i (w_k^i - w_\star^i) \\
&= \tilde{\xi}_k^\top (A^\top P A - \tau^2 P) \tilde{\xi}_k + \tilde{v}_k^\top \hat{B}^\top P \hat{B} \tilde{v}_k + e_k^\top E^\top P E e_k \\
&\quad + 2 \left( \tilde{v}_k^\top \hat{B}^\top P \hat{A} \tilde{\xi}_k + e_k^\top E^\top P \hat{A} \tilde{\xi}_k + \tilde{v}_k^\top \hat{B}^\top P E e_k \right) \\
&\quad + \sum_{i=1}^2 \lambda^i \left( \tilde{\xi}_k^\top \hat{C}^{i\top} M^i \hat{C}^i \tilde{\xi}_k + \tilde{v}_k^\top \hat{D}^{i\top} M^i \hat{D}^i \tilde{v}_k + e_k^\top E^{i\top} M^i E^i e_k \right) \\
&\quad + 2 \sum_{i=1}^2 \lambda^i \left( \tilde{v}_k^\top \hat{D}^{i\top} M^i \hat{C}^i \tilde{\xi}_k + e_k^\top E^{i\top} M^i \hat{C}^i \tilde{\xi}_k + \tilde{v}_k^\top \hat{D}^{i\top} M^i E^i e_k \right),
\end{aligned} \tag{28}$$

where  $\tilde{\xi}_k = \xi_k - \xi_\star$ , and  $\tilde{v}_k = v_k - v_\star$ , for simplicity. We now apply Young's inequality on the cross terms in (28), which yields

$$\begin{aligned}
& V_{k+1} - \tau^2 V_k + \sum_{i=1}^2 \lambda^i (w_k^i - w_\star^i)^\top M^i (w_k^i - w_\star^i) \\
&\leq \tilde{\xi}_k^\top (A^\top P A - \tau^2 P) \tilde{\xi}_k + \tilde{v}_k^\top \hat{B}^\top P \hat{B} \tilde{v}_k + e_k^\top E^\top P E e_k + 2 \tilde{v}_k^\top \hat{B}^\top P \hat{A} \tilde{\xi}_k \\
&\quad + \gamma^2 (\tilde{v}_k^\top \hat{B}^\top P \hat{B} \tilde{v}_k) + \frac{1}{\gamma^2} (e_k^\top E^\top P E e_k) + \gamma^1 (\tilde{\xi}_k^\top \hat{A}^\top P \hat{A} \tilde{\xi}_k) + \frac{1}{\gamma^1} (e_k^\top E^\top P E e_k) \\
&\quad + \sum_{i=1}^2 \lambda^i \left( \tilde{\xi}_k^\top \hat{C}^{i\top} M^i \hat{C}^i \tilde{\xi}_k + \tilde{v}_k^\top \hat{D}^{i\top} M^i \hat{D}^i \tilde{v}_k + e_k^\top E^{i\top} M^i E^i e_k + 2 \left( \tilde{v}_k^\top \hat{D}^{i\top} M^i \hat{C}^i \tilde{\xi}_k \right) \right) \\
&\quad + \sum_{i=1}^2 \lambda^i \left( \gamma^4 \tilde{v}_k^\top \hat{D}^{i\top} M^i \hat{D}^i \tilde{v}_k + \frac{1}{\gamma^4} e_k^\top E^{i\top} M^i E^i e_k + \gamma^3 \tilde{\xi}_k^\top \hat{C}^{i\top} M^i \hat{C}^i \tilde{\xi}_k + \frac{1}{\gamma^3} e_k^\top E^{i\top} M^i E^i e_k \right).
\end{aligned} \tag{29}$$

If we rearrange the right-hand side of the inequality in matrix form, we obtain,

$$\begin{aligned}
& V_{k+1} - \tau^2 V_k + \sum_{i=1}^2 \lambda^i (w_k^i - w_\star^i)^\top M^i (w_k^i - w_\star^i) \leq \\
& \left[ \begin{array}{c} \tilde{\xi}_k^\top \\ \tilde{v}_k^\top \end{array} \right] \left( \left[ \begin{array}{cc} (1 + \gamma^1) \hat{A}^\top P \hat{A} - \tau^2 P & \hat{A}^\top P \hat{B} \\ \hat{B}^\top P \hat{A} & (1 + \gamma^2) \hat{B}^\top P \hat{B} \end{array} \right] \right. \\
& \quad \left. + \left[ \begin{array}{c} \hat{C}^1 \ \hat{D}^1 \\ \hat{C}^2 \ \hat{D}^2 \end{array} \right]^\top \left[ \begin{array}{cc} \lambda^1 M^1 (1 + \gamma^3) & 0 \\ 0 & \lambda^2 M^2 (1 + \gamma^4) \end{array} \right] \left[ \begin{array}{c} \hat{C}^1 \ \hat{D}^1 \\ \hat{C}^2 \ \hat{D}^2 \end{array} \right] \right) \left[ \begin{array}{c} \tilde{\xi}_k \\ \tilde{v}_k \end{array} \right] \\
& \quad + e_k^\top \left( \left( 1 + \frac{1}{\gamma^1} + \frac{1}{\gamma^2} \right) E^\top P E + \sum_{i=1}^2 \lambda^i \left( 1 + \frac{1}{\gamma^3} + \frac{1}{\gamma^4} \right) E^{i\top} M^i E^i \right) e_k.
\end{aligned} \tag{30}$$

The fact that the linear matrix inequality (25) is satisfied proves the claim. Furthermore, we conclude that  $\sum_{i=1}^2 \lambda^i (w_k^i - w_\star^i)^\top M^i (w_k^i - w_\star^i) \geq 0$  from Lemma C.1 and C.2. This simplifies the previous expression to

$$V_{k+1} \leq \tau^2 V_k + e_k^\top Q e_k,$$

where we have also inserted the definition of the matrix  $Q$ . The right-hand side can further be bounded by virtue of the reset mechanism and the event-based communication, which results in

$$V_{k+1} \leq \tau^2 V_k + \bar{\sigma}(Q) \Delta^2. \tag{31}$$

We are now in a position where we can apply Lemma C.4, which concludes

$$V_k \leq \tau^{2k} V_0 + \frac{\bar{\sigma}(Q)\Delta^2}{1 - \tau^2}.$$

By definition of the quadratic storage function we conclude

$$|\xi_k - \xi_*|^2 \leq \tau^{2k} \frac{\bar{\sigma}(P)}{\underline{\sigma}(P)} |\xi_0 - \xi_*|^2 + \frac{\bar{\sigma}(Q)\Delta^2}{\underline{\sigma}(P)(1 - \tau^2)},$$

which implies the result of Thm. C.5. □

## D Bound on Event-Based Error Variables

**Proposition D.1.** *Let  $f$  be  $L$ -smooth and convex and let  $\{z \in \mathbb{R}^n \mid g(z) < \infty\}$  be contained in a ball of radius  $R$ . Then, the disturbances  $\chi_k^{di}$  and  $\chi_k^{zi}$  are bounded by*

$$|\chi_k^{zi}| \leq 2R, \quad |\chi_k^{di}| \leq (\alpha + 1) \frac{2(\rho + L)}{\rho} |x_*^i| + 2R,$$

for all  $i = 1, \dots, N$  and all  $k \geq 0$ , where  $x_*^i := \arg \min_{x \in \mathbb{R}^n} f^i(x) + \rho|x|^2/2$ , and where  $\chi_k^{zi}$  denotes the communication drops when communicating  $z_k$  between agent  $N + 1$  and agent  $i$ .

*Proof.* Due to the assumption that the domain of  $g$  is contained in a ball of radius  $R$ , we conclude  $|z_k| \leq R$  for all  $k \geq 0$ . This also implies that  $|\hat{z}_k^i| \leq R$  and concludes the bound on  $\bar{\chi}^z$ . For obtaining the remaining two bounds, we analyze the  $x^i, u^i$  dynamics of agent  $i$ , where we introduce the convex conjugate

$$\bar{f}^i(u, z) = \sup_{x \in \mathbb{R}^n} u^\top x - f^i(x) - \frac{\rho}{2}|x - z|^2.$$

We note that the supremum is attained for  $x_{k+1}^i$ , if  $u = -\rho u_k^i$  and  $z = \hat{z}_k^i$  in the previous equation. In addition, due to the properties of the convex conjugate, we conclude that  $\bar{f}^i(\cdot, z)$  is  $1/\rho$ -smooth and  $1/(\rho + L)$ -strongly convex. The conjugate subgradient theorem implies,

$$\nabla_u \bar{f}^i(-\rho u_k^i, \hat{z}_k^i) = x_{k+1}^i,$$

which means that the updates for  $u_k^i$  can now be expressed as:

$$u_{k+1}^i = u_k^i + \nabla_u \bar{f}^i(-\rho u_k^i, \hat{z}_k^i) - \hat{z}_k^i.$$

By applying Taylor's theorem, we obtain

$$u_{k+1}^i = u_k^i + \nabla_u^2 \bar{f}^i(\nu_k, \hat{z}_k^i)(-\rho u_k^i) - \hat{z}_k^i + \nabla_u \bar{f}^i(0, \hat{z}_k^i),$$

for some  $\nu_k \in \mathbb{R}^n$ . By leveraging the fact that, as a result of strong convexity and smoothness of  $\bar{f}^i(\cdot, z)$ , the Hessian  $\nabla_u^2 \bar{f}^i(\cdot, z)$  is upper and lower bounded by  $1/\rho$  and  $1/(\rho + L)$ , respectively, we conclude

$$|u_{k+1}^i| \leq \left(1 - \frac{\rho}{\rho + L}\right) |u_k^i| + |\hat{z}_k^i - \nabla_u \bar{f}^i(0, \hat{z}_k^i)|. \quad (32)$$

By a similar argument based on Taylor's theorem, we can bound the last term in the previous equation by

$$|\hat{z}_k^i - \nabla_u \bar{f}^i(0, \hat{z}_k^i)| \leq |x_*^i| + \frac{L}{\rho + L} |\hat{z}_k^i|.$$

Unrolling the recursion in (32) and exploiting the fact that  $u_0^i = 0$  yields

$$|u_k^i| \leq \frac{\rho + L}{\rho} |x_*^i| + \sup_{k \geq 0} |\hat{z}_k^i|,$$

where the last term is bounded by  $R$ . Finally, due to the  $1/\rho$ -smoothness of  $\bar{f}^i(\cdot, z)$ , we conclude  $|x_{k+1}^i| \leq |u_k^i|$ , which yields the desired result as follows,

$$\begin{aligned} |\chi^{di}| &= |\alpha x_{k+1}^i + u_k^i| \leq \alpha |x_{k+1}^i| + |u_k^i| \leq (\alpha + 1) |u_k^i| \leq (\alpha + 1) \left( \frac{\rho + L}{\rho} |x_*^i| + \sup_{k \geq 0} |\hat{z}_k^i| \right) \\ &\leq (\alpha + 1) \left( \frac{\rho + L}{\rho} |x_*^i| + R \right). \end{aligned}$$

□

## E Diminishing Communication Threshold

In the main text, we focused our presentation on fixed communication thresholds. However, it is important to note that our approach and our analysis can be easily extended to the case where communication thresholds  $\Delta$  are varied as a function of the number of iterations. For example, it is straightforward to show that for any vanishing sequence  $\Delta_k$ , our iterates indeed converge to the minimizer of (2).

**Corollary E.1.** *Let the assumptions of Thm. C.5 be satisfied and let  $\Delta_k \geq 0$  be such that  $\Delta_k \rightarrow 0$  for  $k \rightarrow \infty$ . Then  $\lim_{k \rightarrow \infty} |\xi_k - \xi_*|^2 \rightarrow 0$ .*

*Proof.* According to Thm. C.5, the following holds,

$$V_{k+1} \leq \tau^2 V_k + \bar{\sigma}(Q) \Delta_k^2,$$

see (31). We now apply Lemma 3 in Sec. 2.2 in [Polyak, 1987], which yields the desired result.  $\square$

We can also derive an explicit convergence rate. In fact, the following corollary proves that if  $\Delta_k^2$  is the form  $q/(k+1)^t$ , where  $q > 0$  and  $t > 0$  are constants and  $k$  is the iteration number,  $|\xi_k - \xi_*|^2$  converges at a rate of  $\mathcal{O}(1/k^t)$ .

**Corollary E.2.** *Let the assumptions of Thm. C.5 be satisfied and let  $\Delta_k^2 \leq \frac{q}{(k+1)^t}$ ,  $\forall k \geq 0$ ,  $t > 0$ . Then, the following holds for all  $k \geq 0$ :*

$$|\xi_k - \xi_*|^2 \leq \frac{1}{\underline{\sigma}(P)} \left( \frac{k_0}{k + k_0} \right)^t c_0,$$

where  $k_0 = \frac{1}{\left(\frac{2}{1+\tau^2}\right)^t - 1}$  and  $c_0 = \max \left\{ \frac{2\bar{\sigma}(Q)q}{1-\tau^2}, \bar{\sigma}(P) |\xi_0 - \xi_*|^2 \right\}$ .

*Proof.* According to (31), the following holds,

$$V_{k+1} \leq \tau^2 V_k + \bar{\sigma}(Q) \frac{q}{(k+1)^t}.$$

We make the following claim:

$$V_k \leq c_0 \left( \frac{k_0}{k + k_0} \right)^t, \quad \forall k \geq 0.$$

We prove the claim by induction. The claim holds for  $k = 0$  due to the fact that  $c_0 \geq \bar{\sigma}(P) |\xi_0 - \xi_*|^2$ . We therefore assume that the claim holds for  $k$  and show that this implies that the claim holds for  $k + 1$ . This yields

$$\begin{aligned} V_{k+1} &\leq \tau^2 V_k + \bar{\sigma}(Q) \frac{q}{(k+1)^t} \\ &\leq \tau^2 c_0 \left( \frac{k_0}{k + k_0} \right)^t + \bar{\sigma}(Q) \frac{q}{(k+1)^t} \\ &\leq c_0 \left( \frac{k_0}{k + k_0 + 1} \right)^t \left( \tau^2 \left( \frac{k + k_0 + 1}{k + k_0} \right)^t + \frac{\bar{\sigma}(Q)q}{c_0 k_0^t} \left( \frac{k + k_0 + 1}{k + 1} \right)^t \right) \\ &\leq c_0 \left( \frac{k_0}{k + k_0 + 1} \right)^t \left( \tau^2 \left( \frac{k_0 + 1}{k_0} \right)^t + \frac{\bar{\sigma}(Q)q}{c_0} \left( \frac{k_0 + 1}{k_0} \right)^t \right) \\ &\leq c_0 \left( \frac{k_0}{k + k_0 + 1} \right)^t, \end{aligned}$$

and completes the induction argument.  $\square$



## F Additional Experiments and Hyperparameters

We ran various experiments in order to assess the performance of the event-based distributed learning algorithm (Alg. 1). In the comparative studies, we choose FedAvg [McMahan et al., 2017], FedProx [Li et al., 2020a], FedADMM [Zhou and Li, 2023] as baselines, since these methods have been developed to address challenges such as data heterogeneity and communication efficiency. For a fair comparison in terms of computation resources in all setups, each of the agents are run for the same number of local gradient steps.

We include the first example in Sec. 5, which showcases how an MNIST Classifier can be trained in a distributed and communication efficient way. We now proceed to describe the details of the experiment. Our setup includes ten agents, where each agent stores the training data of a different digit, which results in data distributions among agents that are largely different.

We train our model using Alg. 1, where we replace the full minimization step of each local objective with five steps of stochastic gradient descent with a learning rate of  $l_r = 10^{-1}$ . Further hyperparameters are listed in Tab. 1. As can be seen from Fig. 3, our method based on event-based communication outperforms the other baselines.

Table 1: The table summarizes the hyperparameters used for distributed training of MNIST classifier (Fig. 3).

Hyperparameter	Value
number of agents ( $N$ )	10
size of neural network layers	[400, 200, 10]
learning rate (gradient descent step-size)	0.1
number of iterations	100
$\Delta^d = \Delta, \Delta^z = 0.1 \times \Delta$	range between [0, 10]
$\mu$ (FedProx)	0.1
$\rho$ (FedADMM, Alg. 1)	1

The next sections provide additional numerical experiments. We first show an example based on LASSO where the local objectives are strongly convex (Sec. F.1 and F.2). In this setup, our theoretical results apply. Sec. F.3 demonstrates the scalability of our algorithm for training larger models by training a convolutional network on the CIFAR-10 dataset. Last but not least, Sec. A.2 shows how our algorithm can train an MNIST classifier, when only local communications are allowed, as specified by a given communication graph. In such a setup, the baselines FedAvg, FedProx and FedADMM are not applicable.

### F.1 Linear Regression and LASSO with Non-i.i.d. Data

We conduct numerical experiments based on the following distributed learning problem:

$$\begin{aligned} \min_{x \in \mathbb{R}^n, z \in \mathbb{R}^n} \quad & \sum_{i=1}^N \frac{1}{2} |A^i x^i - b^i|^2 + \lambda |z|_1, \\ \text{subject to} \quad & x^i - z = 0, \quad i = 1, \dots, N, \end{aligned} \tag{33}$$

where  $A^i \in \mathbb{R}^{m \times n}$ ,  $b^i \in \mathbb{R}^m$ . In the data generation process, we generate samples from three different distributions: a standard normal distribution, a Student's t distribution with one degree of freedom, and a uniform distribution in the range  $[-5, 5]$ . These samples are concatenated to form a single dataset, which is then partitioned into subsets for each agent  $i$  to obtain  $(A^i, b^i)$ . Finally, we normalize the feature vectors and target values for each agent to prepare the data for the learning problem. In this non-i.i.d. setting, local optimal points of individual agents  $x_*^i$  are far away from each other, and their average  $\sum_{i=1}^N x_*^i / N$  is also far away from the global optima  $x_*$ . The experiments were run for  $T_{\max} = 50$  steps, which are required for Alg. 1 to converge to the global optimal point with high precision. Fig. 8 illustrates the communication load against the absolute difference between the objective function value  $f$  and the optimal value  $f^*$ , where the communication load is defined as the number of communications accumulated over time.

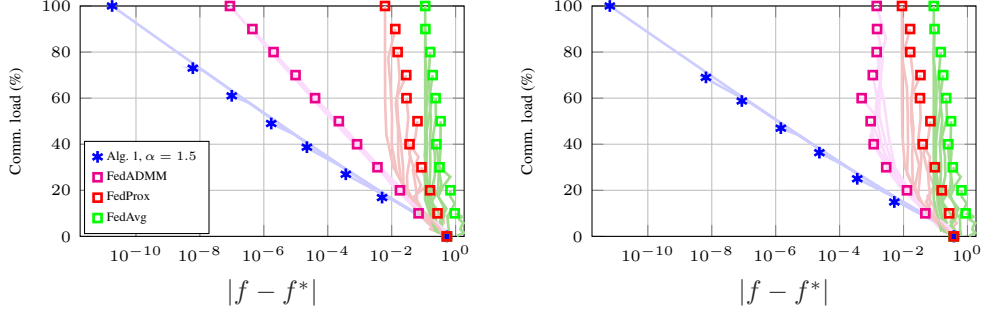


Figure 8: The figure shows the communication load versus accuracy trade-off for the different methods applied to two distinct problems derived from (33): linear regression ( $\lambda = 0$ , left panel), and on the right, LASSO ( $\lambda = 0.1$ , right panel).

In the first scenario, we set  $\lambda = 0$  to obtain a linear regression problem, where the proposed algorithm with relaxation parameter  $\alpha = 1.5$  clearly outperforms the baseline methods. We note that the gap between the global and local optimal points prevents FedAvg and FedProx from converging to the optimal point  $f^*$ .

For the second case, we set  $\lambda = 0.1$  to solve the LASSO problem. By assumption, FedAvg and FedADMM require the local objective functions to be smooth. However, we allow handling nonsmooth local objective functions, which is relevant to the distributed learning problems with  $\ell^1$  regularization. To avoid a noncontinuous gradient for the local minimization FedADMM, FedAvg and FedProx, the local update step is carried out by the following local gradient,

$$\nabla_{x^i} \tilde{f}^i(x^i) = A^{i\top} (A^i x^i - b^i) + \frac{\lambda}{N} \begin{cases} \text{sgn}(x^i) & |x^i| > \delta \\ \frac{1}{\delta} x^i & |x^i| \leq \delta \end{cases}, \quad (34)$$

where  $\delta$  can be chosen as small as  $1e - 16$  (double precision machine epsilon). However, we found that the results are largely unaffected by the choice of  $\delta$ .

Table 2: The table summarizes the hyperparameters used for the distributed linear regression and LASSO experiments (Fig. 8).

Hyperparameter	Value
number of agents ( $N$ )	50
augmented lagrangian parameter ( $\rho$ )	1
gradient descent step-size	1
number of iterations	50
$\Delta^d = \Delta^z = \Delta$	range between $[0, 10^{-2}]$

## F.2 Effect of Communication Drops

To observe the effect of communication drops, we repeated the same LASSO experiment in (33) with hyperparameters in Tab. 3, but this time, we allow the transmission of information from the agents to the server to fail with a probability of 0.3. As seen in the second panel of Fig. 9, if we have no reset, i.e.,  $T = \infty$ , the algorithm cannot converge and a significant error remains. On the left panel, the trade-off between communication load and suboptimality is presented. More frequent reset operations lead to a faster convergence and less error, in exchange for additional communication cost that comes with the reset.

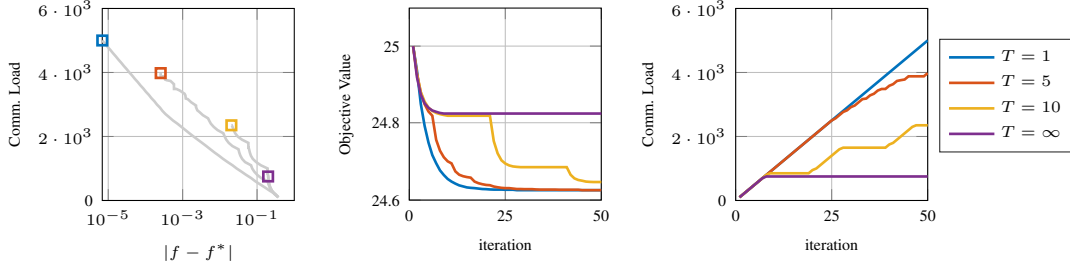


Figure 9: The left panel presents the trajectory of communication load versus suboptimality of the objective function value. The panel in the center shows the evolution of the objective function for different values of the reset period for a drop rate of 0.3 and for  $\Delta = 10^{-3}$ , whereas the right panel shows the cumulative communication load over time in addition to the reset communication at each  $T$  step.

Table 3: The table summarizes the hyperparameters used for the distributed LASSO experiment against communication drops (Fig. 9).

Hyperparameter	Value
number of agents ( $N$ )	50
L1 regularization parameter ( $\lambda$ )	0.1
augmented lagrangian parameter ( $\rho$ )	1
relaxation parameter ( $\alpha$ )	1
gradient descent step-size	1
number of iterations	50
$\Delta^d = \Delta^z = \Delta$	$10^{-3}$

### F.3 Image Classifier for CIFAR-10

We also apply our implementation to compute a CIFAR-10 classifier [Krizhevsky, 2009] in a distributed setting. The data are distributed among ten agents according to a Dirichlet distribution, i.e., we sample  $p_a \sim \text{Dir}_N(\beta)$ , where  $N$  is the number of agents and  $\beta = 0.5$ . We then assign a  $p_{a,j}$  proportion of the training data class  $a$  to the agent  $j$ .

The classifier model is given by a CNN with 4 convolutional layers, each with  $3 \times 3$  kernels and 32, 64, 128 and 256 filters respectively and three fully connected layers with ReLU activation functions. After each set of convolutions, there is a  $2 \times 2$  max pooling layer followed by a ReLU activation.

We set the communication threshold for the server to zero ( $\Delta^z = 0$ ), allowing the server to broadcast its state ( $z$ ) at each round. In this setting, the total communication load is calculated only by counting the number of communications triggered by the agents and normalized according to the full communication case. Our experimental results shown in Fig. 10 highlight that our event-based communication strategy can indeed be implemented for solving large-scale problems. We also conclude that communication cost can be reduced by more than 50% without significantly degrading the resulting classification accuracy.

### F.4 Distributed Training on a Graph

Our distributed learning algorithm, Alg. 2, is general enough to train a machine learning classifier over a network of agents; the network structure can be encoded by a proper selection of the linear constraint matrices  $A$  and  $B$  (see App. A for further details). Our framework therefore generalizes well beyond server-client structures, and our theoretical analysis also captures the influence of the network structure on the resulting convergence rate.

In order to highlight the versatility, we train an MNIST Classifier over a network of agents. We use a multi-layer perceptron that has the same structure as in Sec. 5 and consider a situation where each agent has only access to the training data of a single digit. Fig. 11 shows the resulting communication

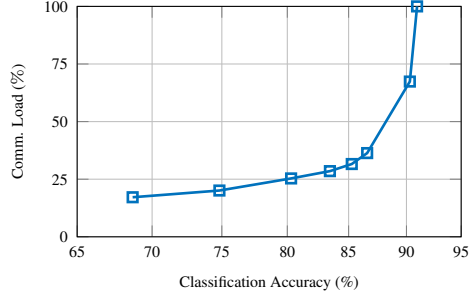


Figure 10: The figure shows the trade-off between total communication load and classification accuracy on the CIFAR-10 dataset.

Table 4: The table summarizes the hyperparameters used for the distributed learning of a CIFAR-10 classifier (Fig. 10).

Hyperparameter	Value
number of agents ( $N$ )	10
augmented lagrangian parameter ( $\rho$ )	0.01
learning rate	0.01
momentum	0.9
number of iterations	40
number of local epochs	8
batch size	64
$\Delta^d$	range between $[0, 22]$

load and classification accuracy trade-off on the entire dataset (left), whereas the diagram on the right shows the network structure (only communication along the edges of the graph is allowed). The error bars indicate the range (minimum and maximum) of the classification accuracy among the different agents.

The results shown in Fig. 11 and highlight that a purely random selection of agents (suggested in [Yu and Freris, 2023]) results in a worse trade-off curve, which further motivates our event-based strategy. We also apply our algorithm to a much larger distributed learning problem with 50 agents and where the corresponding accuracy versus communication trade-off is shown in Fig. 12, together with the agent network that has been used.

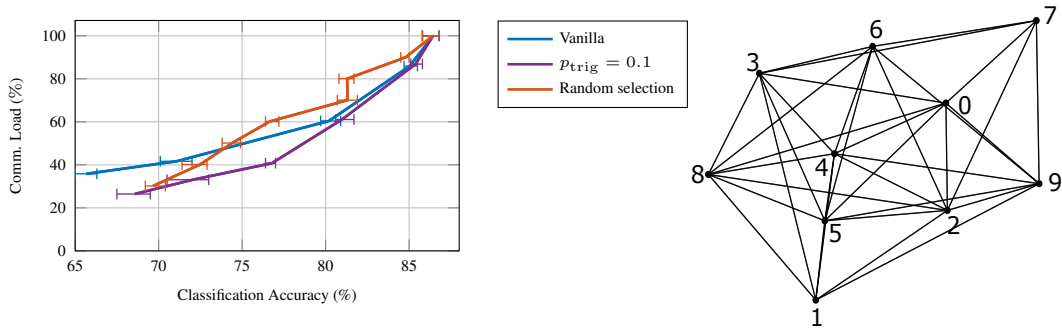


Figure 11: The figure shows a comparison of the vanilla event-based and the randomized event-based communication strategy (see Sec. 2) with a purely random selection of agents. The outcome of a purely random strategy is consistently worse with respect to the resulting trade-off between communication load and classification accuracy. The right panel visualizes the agent network with ten agents connected with 70 edges.

Table 5: The table summarizes the hyperparameters used for the distributed training of MNIST classifier over a graph (Fig. 11).

Hyperparameter	Value
number of agents ( $N$ )	10
size of neural network layers	[400, 200, 10]
learning rate (gradient descent step-size)	$5 \times 10^{-3}$
augmented lagrangian parameter ( $\rho$ )	$5 \times 10^{-3}$
number of iterations	$10^3$
number of gradient steps per iteration	5
$\Delta^x$	range between [0.0, 0.2]

Table 6: The table summarizes the hyperparameters used for the distributed linear regression experiment over a graph (Fig. 12).

Hyperparameter	Value
number of agents ( $N$ )	50
augmented lagrangian parameter ( $\rho$ )	$10^{-5}$
number of iterations	$17 \times 10^3$
$\Delta^x$	range between [0, 1]

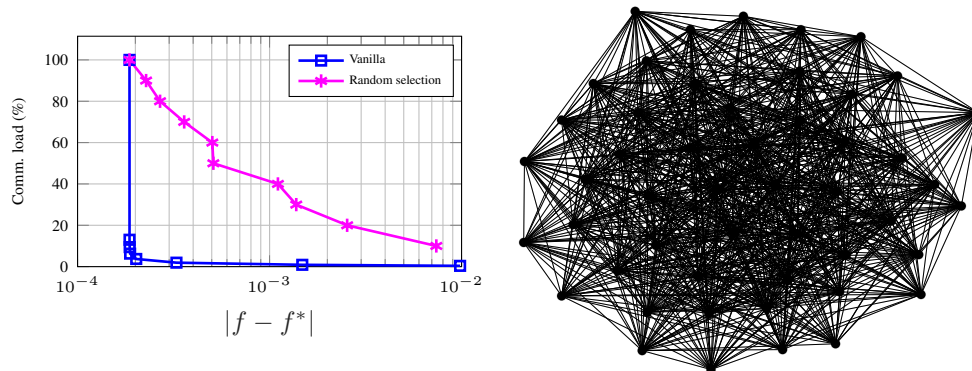


Figure 12: The first panel shows the comparison of the communication load versus solution accuracy for different communication methods applied to the linear regression problem derived from (33) ( $\lambda = 0$ ). The right panel visualizes the agent network with 50 agents connected with 1762 edges.